https://doi.org/10.5194/hess-2020-468
Preprint. Discussion started: 26 October 2020

Hydrology and Earth System Sciences
Discussions

Space variability of hydrological responses of Nature-Based Solutions and the resulting uncertainty

Yangzi Qiu[1], Igor da Silva Rocha Paz[2], Feihu Chen[3], Pierre-Antoine Versini[1], Daniel Schertzer[1], Ioulia Tchiguirinskaia[1]

[1]HM&Co, École des Ponts ParisTech, Université Paris-Est, Champs-sur-Marne,77455, France
[2]Instituto Militar de Engenharia, Rio de Janeiro, 22290-270, Brazil
[3]School of Architecture, Hunan University, Changsha, 410082, China

Correspondence to: Yangzi Qiu (yangzi.qiu@enpc.fr)

Abstract. During the last decades, the urban hydrological cycle has been strongly modified by the built environment, resulting in fast runoff and increasing the risk of waterlogging. Nature-Based Solutions (NBS), which apply green infrastructures, have been more and more widely considered as a sustainable approach for urban stormwater management. However, the assessment of NBS performance still requires further modelling development because of their hydrological responses sensitively depends on the representation of multiscale space variability of both the rainfall and the NBS distribution. Indeed, we initially argue this issue with the help of the multifractal intersection theorem. To illustrate the importance of this question, the spatial heterogeneous distributions of two series of NBS scenarios (porous pavement, rain garden, green roof, and combined) are quantified with the help of their fractal dimension. We point out consequences of their estimates. Then, a fully-distributed and physically-based hydrological model (Multi-Hydro) was applied to consider the studied catchment and these NBS scenarios with a spatial resolution of 10 m under two different types of rainfall: distributed and uniform, and for three rainfall events. These simulations show that the impact of spatial variability of rainfall on the uncertainty of peak flow of NBS scenarios ranges from about 8 % to 17 %, which is more pronounced than those of the total runoff volume. In addition, the spatial variability of the rainfall intensity at the largest rainfall peak responds almost linearly to the uncertainty of the peak flow of NBS scenarios. However, the hydrological responses of NBS scenarios are less affected by the spatial distribution of NBS. Finally, the intersection effects of the spatial variability of rainfall and the spatial arrangement of NBS seem more pronounced for the peak flow of green roof scenarios and the total runoff volume of combined scenarios.

1 Introduction

The increasing of extreme flooding risks seem strongly related to two essential drivers: rapid urbanization and climate change (Lovejoy and Schertzer, 2013). Adapting to climate change and mitigating urban flooding constitute now significant societal

https://doi.org/10.5194/hess-2020-468
Preprint. Discussion started: 26 October 2020


Hydrology and Earth System Sciences
Discussions

challenges (Loukas et al., 2010; Miller and Hutchins, 2017). Impervious surfaces directly connected to grey infrastructures results in rainfall transfer into runoff rapidly, which largely increases the flooding risks, especially in urban watersheds (Fry and Maxwell, 2017; Ercolani et al., 2018). The approach of expanded and upgraded the capacity of the existing drainage system has been proved costly and unsustainable, which is challenging to realize in highly urbanized cites (Qin et al., 2013). Increasing urban resilience to reduce the risk of urban flood has been emphasized in many countries (Kelman, 2015). Nature-Based Solutions (NBS) refer to a sustainable strategy, capable to reduce the influences of human activities on the natural environment, especially efficient for stormwater management (European Commission, 2015; Cohen-Shacham et al., 2016). To some extent, the NBS concept builds on, and supports, the Low Impact Development (LID), Blue and Green Infrastructure (B&GI), and other parallel concepts (Berry et al., 2015; Bozovic et al., 2017). Regarding stormwater management, NBS suggests using a suite of small-scale controlled measures. This often includes bio-retention swale, porous pavement, green roof, rain garden, and rain barrel, because these infrastructures are able to conserve or recover the natural environment of a region (Newcomer et al., 2014).

The hydrological performances of such NBS have been approached in terms of the reduction of total runoff volume and peak flow at the urban catchment scale (Zahmatkesh et al., 2015; Ahiablame and Shakya, 2016; Bloorchian et al., 2016). Generally, the results of a large number of studies are based on lumped or semi-distributed models (Ahiablame et al., 2013; Liu et al., 2015; Massoudieh et al., 2017; Guo et al., 2019). Indeed, as underlined by Fry and Maxwell, (2017), and Her et al., (2017), fully-distributed models are rarely used (Versini et al., 2016; Hu et al., 2017; Versini et al., 2018). Among all these hydrological models, the semi-distributed Storm Water Management Model (SWMM) remains the one that is most frequently used to investigate the impact of NBS on urban runoff and water quality (Sun et al., 2014; Jia et al., 2015; Palla and Gnecco, 2015; Cipolla et al., 2016; Kwak et al., 2016). Nevertheless, Rossman et al., (2010) demonstrated that SWMM has some limitations in reflecting complicated urban catchments, presenting some difficulties to show different hydrological responses to a variety of urban land uses. The study of Burszta-Adamiak and Mrowiec, (2013) confirmed that SWMM is not really explicit for presenting the hydrological responses of catchments with only the help of the percentage of pervious and impervious land covers. These gaps imply strong limitations to the results obtained with the help of lumped and the semi-distributed models. Thus, to make the modelling results more accurate and credible, there is a strong need to use fully-distributed and physically-based models. Indeed, such models should better assess the hydrological performances of NBS on a smaller scale.

Meanwhile, due to the complexity of the small scale rainfall variability and the lack of high-resolution rainfall data, some studies have been devoted to assess the performances of NBS under the simplifying assumption of a uniform rainfall (design storm or data from rain gauges), hence the impact of spatial rainfall variability in the heterogeneous urban context has not been considered (Holman-Dodds et al., 2003; Gilroy and McCuen, 2009; Qin et al., 2013; Versini et al., 2018; Zhu et al., 2019; Guo et al., 2019). However, the hydrological responses of NBS (model outputs) could largely depend on: (i) the highly spatially variable rainfall fields, (ii) the spatial distribution of the NBS, and (iii) the intersection of (i) and (ii), which induce that the performances of NBS scenarios simulated with uniform rainfall or lumped/semi-distributed model may not be entirely

https://doi.org/10.5194/hess-2020-468
Preprint. Discussion started: 26 October 2020


Hydrology and Earth System Sciences
Discussions

convincing. Therefore, such mentioned impacts remain to be investigated, in particular over higher spatial resolutions, by using the space-time rainfall fields together with a fully-distributed model, allowing for heterogeneous NBS scenarios.

In this respect, the main goal of this study is to investigate the uncertainty of hydrological responses in various NBS scenarios resulting from the spatial variability of rainfall and the heterogeneous distribution of NBS at the urban catchment scale, and thus not those associated to the model structure, hypothesis or parameterization for instance. A fully-distributed and physically-based hydrological model (Multi-Hydro (Giangola-Murzyn, 2013; Ichiba et al., 2018)) is applied on a 5.2 km^2 semi-urban catchment in Guyancourt city (France) at 10 m scale. Two different types of rainfall data from three typical rainfall events in the Paris area are used as meteorological inputs: (i) the data retrieved from the polarimetric X-band radar of École des Ponts ParisTech (ENPC), are characterized by some high spatial and temporal resolutions, which are called the distributed rainfall data; and (ii) the corresponding uniform rainfall data, obtained by spatial averaging of the distributed rainfall data at each time step. The spatial heterogeneity of NBS is grasped by different landuse scenarios, characterized with the help of an across-scale indicator, the fractal dimension. These variability and resulting uncertainties in hydrological responses of the catchment are quantified by considering the peak flow and the total runoff volume in the drainage conduits. It is important to mention here that a precise quantitative evaluation of NBS performances, e.g., peak discharge reduction, total runoff volume reduction, or both, is not the goal of the present study. The authors aim first to deepen the knowledge on the impact of spatial variability of the rainfall on hydrological responses of several NBS scenarios, and that in turn helps to clarify whether the Nature-Based Solutions could be randomly implemented in semi-urban catchments or not.

The organization of this paper is as follows. The next section presents the study area, the rainfall data and the Multi-Hydro model. The details of the NBS scenarios, the framework of modelling experiments and the model validation are described in Section 3. Then, the obtained results are discussed in Section 4. Finally, the main conclusions are summarized in Section 5.

2 Study context, data and methods

2.1 The choice of the case study

This study is conducted on a semi-urban catchment, a part of the city of Guyancourt (France), located on the Saclay Plateau in the southwest suburb of Paris (Fig. 1). The available raw 25-m resolution Digital Elevation Model (DEM) obtained from the French National Institute of Forest and Geographic Information (IGN), which presents the whole catchment, is relatively flat (see the left side of Fig.1). The altitude in the North is slightly higher than that of the South. The highest altitude in the whole catchment reaches 175.1 m, while the lowest one of 143.39 m corresponds to the location of the storage basin (i.e., the outlet of the catchment: Etang des Roussières). The most recent statistical report of Météo-France (2020) indicates that the area is characterized by an oceanic climate with an average annual temperature of about 10.7 ℃ and total annual precipitation around 695 mm. In this context, the Guyancourt catchment is an interesting and appropriate case study for several reasons.

Firstly, Guyancourt is one of the sub-catchments in the upstream of the 34.6 km long Bièvre River, which flows through several increasingly urbanized areas and joins the Seine River in Paris. Bièvre River is well-known by its drastic contribution

https://doi.org/10.5194/hess-2020-468
Preprint. Discussion started: 26 October 2020


Hydrology and Earth System Sciences
Discussions

to the historical 1910 flood in Paris and still easily generates flash floods during the heavy rainfall events (e.g., two severe floods occurred in 1973 and 1982). Therefore, the case of Guyancourt has a reference significance for the Paris region.

Secondly, the Guyancourt city is expected to become a part of the "French Silicon Valley", which currently undergoes a rapid urbanization process over its total area of around 5.2 km^2, with a population of about 30,000 (INSEE 2020). Based on the data from IGN, the current land use of the study area consists of seven main types, including road, parking, building, gully, forest, grass, and water. In total, these seven land use types cover 9.6 %, 10.6 %, 15.5 %, 1.9 %, 28.8 %, 32.7 %, and 0.9 % of the total area, respectively, as shown on the left side of Fig. 2. Currently, the pervious surface accounts for 62.4 % of the total area, and the corresponding impervious surface is 37.6%.

The local authority, the agglomeration community of Saint-Quentin-en-Yvelines ("La communauté d'agglomération de Saint-Quentin-en-Yveline"), manages the urban drainage system of the catchment and provided some related data (right side of Fig. 2). The total length of the drainage system is about 76 km and consists of 4,474 nodes and 4,534 conduits. Overall, the drainage system was designed with a capacity characterized by a return period ranging from 2 to 10 years. The diameters of conduits range between 0.1 m to 1.6 m, 70 % of them between 0.3 to 0.5 m (marked with a yellow line in right side of Fig. 2). The conduits with a diameter ranging between 0.9 to 1.6 m (marked with a purple line in right side of Fig. 2) are the primary conduits, which converge the flow to the storage basin and the outlet.

However, due to climate change, a clear tendency towards growing number of somewhat shorter, but much heavier rainfall events, was perceived for this region (Hoang et al., 2010), causing in recent years a large amount of fast surface runoff and higher peak flow rates. The existing stormwater drainage system may not be able to sustain the future modifications of the watershed, and some low-lying areas in the catchment could suffer more easily from waterlogging, even during moderate rainfalls. As displays Fig. 1, some vulnerable areas and buildings prone to a risk of waterlogging were defined in the Guyancourt catchment by using the ModelBuilder of ArcGIS software (a geoprocessing model for identifying landscape sinks [https://learn.arcgis.com/en/]). In this figure, the blue spots represent the low-lying areas with a total area of 0.6 km^2 that can be easily flooded by stormwater (average rainfall depth of 53 mm). Correspondingly, the yellow spots indicate the vulnerable buildings that lie within or adjacent to these areas.

Thirdly, the local authority installed a gauge at the storage basin (outlet) to monitor water levels, which provided a measurement point of the Guyancourt catchment.

Overall, the relative complexity of the catchment makes it a typical "case study" for analysing some of the uncertainties related to hydrological responses of NBS scenarios, aiming to help the local authorities to find more reasonable and ecological alternatives for future urban planning.

2.2 Rainfall data

In this study, one of the purposes is to assess the impact of spatial variability of rainfall on the hydrological responses of some NBS scenarios. Hence, two kinds of rainfall data were prepared as meteorological inputs: distributed and uniform. The distributed rainfall data were retrieved from the polarimetric X-band radar, located in ENPC, Champs-sur-Marne (East of Paris,

https://doi.org/10.5194/hess-2020-468
Preprint. Discussion started: 26 October 2020


Hydrology and Earth System Sciences
Discussions

France). The distance between the X-band radar and the catchment is around 45 km (see Fig. 1). The spatial and temporal resolutions of the X-band radar are 250 m and 3.4 min, respectively. Three relatively long rainfall events (EV1, EV2, and EV3) with different characteristics that occurred in 2015 were chosen for the study (see Table 1 for more details). Figure 3 (top) shows the maps of rainfall intensity (per radar pixel) at the largest rainfall peak for these three events. The maximum rainfall intensity per pixel is 41.2, 29.1, and 55.6 mm h^{-1}, respectively. To establish a link with classical approaches (e.g., Hamidi et al. (2018)), the standard deviation (*SD*) was used to quantify the variability of the rainfall fields. As presented in Table.1, the *SD* of the rainfall intensity at the largest rainfall peak of the three rainfall events is 4.31, 6.11, and 5.75 mm h^{-1}, respectively. This illustrates that while the strongest rainfall intensity was observed during the EV3, the highest variability of rainfall intensity occurred in the EV2. Figure 3 (middle) presents the total (cumulative) rainfall depth (per radar pixel) for the three rainfall events. The maximum cumulative rainfall per pixel is 36.9, 14.1, and 25.4 mm, respectively. The *SD* of the total rainfall depth of the three rainfall events is 1.21, 0.82, and 1.35 mm, respectively. This demonstrates that the spatial distributions of cumulative rainfall are much less variable compared to those of the rainfall intensity at the peak, with the highest variability computed for the EV3.

The three spatially uniform rainfall events (EV1U, EV2U and EV3U) were constructed by spatial averaging over the whole catchment of original (distributed) rainfall fields at each time step. Figure 3 (bottom) presents the time evolution of the corresponding rainfall rates and cumulative rainfall depths. Each of these events is sufficiently long to contain several rainfall peaks and dry periods. For EV1U, the highest rainfall intensity reaches 20 mm h^{-1}, and the total rainfall accumulates (around 31.5 mm) fastly between the first and the third rainfall periods (approximately 24 h). The maximum rainfall intensity of the EV2U and EV3U is 9 mm h^{-1} and 36.4 mm h^{-1}, and the total rainfall amounts about 12 mm and 20 mm, respectively. Although the largest rainfall peak of the EV3U is 36.4 mm h^{-1}, it lasted only for 3 min, just sufficient to contribute about 10 % to the total rainfall depths.

Overall, this initial analysis suggests that in spite of some very similar characteristics, the selected events cover a truly wide spectrum of rainfall space-time variability.

2.3 Multi-Hydro model

The Multi-Hydro model is a fully-distributed and physically-based hydrological model, which has been developed by HM&Co/ENPC (El Tabach et al., 2009; Giangola-Murzyn, 2013; Ichiba, 2016; Ichiba et al., 2018). It has been successfully implemented and validated in several catchments (e.g., Versini et al., 2016; Ichiba et al., 2017; Gires et al., 2017; Gires et al., 2018; Alves de Souza et al., 2018; Versini et al., 2018; Paz et al., 2019). In this study, it is used for assessing hydrological responses of the NBS scenarios at the urban catchment scale.

Multi-Hydro constitutes the interactive core among the four open-source modules (rainfall, surface runoff, drainage, and infiltration) that represent essential elements of the hydrological cycle in urban environment.

https://doi.org/10.5194/hess-2020-468
Preprint. Discussion started: 26 October 2020


Hydrology and Earth System Sciences
Discussions

The rainfall module (MHRC) can treat different kinds of rainfall data (from radar or rain gauge). In order to adapt the rainfall inputs for Multi-Hydro, the intersection between the pixels of the model (with a 10 m spatial resolution in this study) and the pixels of the X-band radar data (with a 250 m spatial resolution) were performed by the QGIS interface using the following equation (Paz et al., 2018):

$$R_{i_{MH10m},j_{MH10m}} = \frac{\sum_{i_{250m},j_{250m}}\left[R_{i_{250m},j_{250m}}\cdot\left(A_{i_{10m},j_{10m}} \cap A_{i_{250m},j_{250m}}\right)\right]}{\sum_{i_{250m},j_{250m}}\left(A_{i_{10m},j_{10m}} \cap A_{i_{250m},j_{250m}}\right)} \quad (1)$$

where $R_{i_{MH10m},j_{MH10m}}$ is the rainfall rate computed for each pixel of the model; $R_{i_{250m},j_{250m}}$ is the rainfall rate of X-band radar data in each pixel; $A_{i_{10m},j_{10m}}$, $A_{i_{250m},j_{250m}}$ is the area of each pixel of the model and the X-band radar data, respectively.

The surface module (MHSC) of Multi-Hydro uses the code of the Two-Dimensional Runoff Erosion and Export (TREX) model that computes the surface runoff and infiltration at each pixel, depending on the land use classification (Velleux et al., 2008). The diffusive wave approximation of the Saint-Venant equations is used for calculating the overland flow, following the conservation of mass and momentum equations. The groundwater module (MHGC) is based on the Variably Saturated and 2-Dimensional Transport (VS2DT) model, which simulates the process of infiltration in the unsaturated subsurface zone. For a simplification of the NBS scenarios, this module is not applied in this study. The drainage module (MHDC) in Multi-Hydro uses the code of 1D SWMM model (James et al., 2010) to simulate the sewer network. This model represents the flow computed by 1D Saint-Venant equations in conduits and nodes.

The high spatial resolution of Multi-Hydro allows an easy implementation of small-scale controlled measures, like the rain garden, green roof, bio-retention swale, porous pavement, and rainwater tank, by locally modifying the land use parameters to link the size and shape of the corresponding NBS infrastructures, with their infiltration and storage capacities.

3 Numerical investigation of the NBS scenarios

3.1 Multi-Hydro implementation in the Guyancourt catchment

Based on the fully distributed character of Multi-Hydro, users can choose a specific spatial resolution. In this study, Multi-Hydro was implemented with a 10 m spatial resolution (the grid system creates square grids with a cell size of 10 m), and a temporal loop of 3 min. The 10 m resolution was performed because it sufficiently represents the heterogeneity of the catchment, and also for saving the computation time.

The implementation of Multi-Hydro in a new catchment starts with the conversion of the original GIS data (e.g., land use, topography) into the standard rasterised format with the desired resolution by using the MH-AssimTool (Richard et al., 2013), a supplementary GIS-based module for generating the input data for Multi-Hydro). During this process, a unique land use class was assigned to each pixel, specifying its hydrological and physical properties. In order to attribute a unique land use class to each pixel, the following priority order was used in this study: gully, road, parking, house, forest, grass, and water surface. Because the gully is the only land use class able to connect the surface module and the drainage module, it has the highest priority (i.e., if a raster pixel contains gully and the other land use classes, the whole pixel will be considered as gully).

https://doi.org/10.5194/hess-2020-468
Preprint. Discussion started: 26 October 2020


Hydrology and Earth System Sciences
Discussions

Generally, this order considers the impervious land use classes have higher priority than the permeable land use classes, which result in an overestimation of impervious land uses (see Ichiba et al., 2017, for an alternative approach). After the rasterization process, the impervious land uses occupied 54 % of the Guyancourt catchment (Fig. 4). In this study, all the standard model parameters related to the land use classification were selected from the Multi-Hydro manual (Giangola-Murzyn et al., 2014), as they are shown in Table 2. Besides the land use, the elevation is also assigned to each pixel, which was obtained by performing the interpolation on the raw DEM information, freely available at the 25m-resolution.

Green roof is a special NBS measure that can be simulated by a specific module in Multi-Hydro (Versini et al., 2016). Accordingly, five physically-based parameters are defined for the green roof. They are based on the experimental site of Cerema (Ile-de-France) where several green roof configurations were monitored (see Versini et al., 2016). In detail, the chosen configuration is the following: substrate thinness of 0.03 m and characterized by a porosity of 39.5%, an initial moisture condition of 10 %, a field capacity of 0.3, and a hydraulic conductivity of 1.2 m h^{-1}.

3.2 Simulation scenarios

For achieving the purpose of the study, a series of NBS scenarios were created and simulated under both different types of rainfall (described in Sect. 2.2). The baseline scenario is considered as the current configuration of the Guyancourt catchment, without implementing any NBS (Fig. 2 left). The baseline scenario will be used later on for the model validation. All details concerning the scenarios of the NBS implementations, including a detailed description of each NBS and the percentage of the space required for its implementation, are presented in Table 3, while the maps of the resulting land use are illustrated on Fig 5.

The first set of NBS scenarios includes porous pavement (PP1), rain garden (RG1), green roof (GR1), and their combined scenario (Combined1). For each scenario, the corresponding NBS are implemented heterogeneously over the catchment, while respecting the local catchment conditions and stormwater management requirements. They are applied to assess the impact of spatial variability of rainfall on the hydrological responses of NBS scenarios.

The second set of NBS scenarios (PP2, RG2, GR2, and Combined2) was proposed with a different arrangement to assess the potential effects of a heterogeneous implementation of NBS at the urban catchment scale. Regarding these two sets of NBS scenarios, the ones related to the same type of NBS (e.g., PP1 and PP2) require the same percentage of the space for their implementation over the whole catchment. But, both scenarios significantly differ in terms of spatial distributions of the considered asset. This distribution is characterized by the across-scale indicator, called fractal dimension presented in details in the following paragraph.

3.2.1 Fractal dimension of NBS scenarios

To quantify the multi-scale space heterogeneity of NBS in each NBS scenario, we applied the concept of fractal dimension (D_F), which was initially introduced to describe the scale invariance of some irregular geometric objects (Mandelbrot, 1983).

https://doi.org/10.5194/hess-2020-468
Preprint. Discussion started: 26 October 2020


Hydrology and Earth System Sciences
Discussions

Namely, a similar structure can be observed in any scale. D_F has been often used in catchment hydrology (e.g., Schertzer and Lovejoy, 1984; Schertzer and Lovejoy, 1987; Schertzer and Lovejoy, 1991; Lavallée et al., 1993; Gires et al., 2013; Gires et al., 2016; Ichiba et al., 2017; Paz et al., 2020; Versini et al., 2020). In this study, a standard box-counting technique was applied to estimate the D_F of each NBS scenario (Hentschel and Procaccia, 1983; Lovejoy et al., 1987). The D_F of a geometrical set A (here represented by the non-overlapping pixels of NBS embedded in a 2-D space) is obtained with the following power-law:

$$N_{\lambda,A} \approx \lambda^{D_F} \quad (2)$$

where $N_{\lambda,A}$ is the number of non-empty (containing NBS) pixels to cover the set A, at the resolution λ, which is defined as the ratio between the outer scale L and the observation scale l ($\lambda = \frac{L}{l}$). The symbol ≈ means an asymptotic relation (i.e. for large resolution λ and possibly up to a proportionality prefactor).

Based on Eq. (2), we count the number of pixels containing at least one NBS, by starting with the smallest pixel size (l = 10 m in this study), then continuously increasing the pixel size by simply merging the 4 adjoined pixels. This procedure is repeated until reaching the largest pixel size (L). Thus, $N_{\lambda,A}$ is counted at different resolutions, and the results are plotted in the log-log plot (see Fig. 6). Corresponding to Eq. (2), the fractal dimension D_F of each NBS scenario is defined as follows:

$$D_F \approx \frac{ln(N_{\lambda,A})}{ln\,\lambda} \quad (3)$$

Here, for each scenario, a square area of 128 x 128 pixels was extracted from the catchment to make the fractal analysis (see the example of the PP1 scenario in Fig. 5). In order to avoid the "no data" areas, which would bias the fractal dimension estimate, the selected square area is the greatest possible size characterized by a multiple of two in the studied catchment.

As shown in Fig. 6, all the NBS scenarios are presented with two scaling behaviour regimes, with a scale break roughly at 80 m. For each regime, the scaling is robust, with linear regression coefficients (R^2) around 0.99. For the first regime corresponding to the small-scale range (10 m – 80 m) that related to the assets implementation level, the dimension D_F is around 1 for most of NBS scenarios. It is in contrast with the second regime, the large-scale range (from 80 m to 1280 m) that exhibits a scaling behaviour with a D_F ranging from about 1.75 to 1.98. We also applied fractal analysis on the impervious surface of the baseline scenario in the same selected area, and we also found the same scale break at 80 m (the D_F of the baseline scenario in each regime are presented in Fig. 6). Therefore, it rather confirms that the spatial distribution of NBS is strongly constrained by the urbanisation level of the catchment.

The D_F of each NBS scenario is summarized in Table 3. The dimension D_F measures the implementation level of NBS across scales. For instance, the D_F (large-scale) of the two combined scenarios (Combined1 and Combined2) is close to 2, showing that NBS are rather homogeneously distributed. However, it is important to notice that, in spite of initially identical percentage at a given scale of the NBS implementation over the catchment, the resulting D_F could be quite different. It is simply because the percentage of the space is a scale dependent quantity, while D_F quantifies the propagation of the spatial heterogeneity for each of NBS scenarios, from the smallest scale to the outer scale of the catchment. This propagation remains scenario dependent and hence a subject to its optimisation.

https://doi.org/10.5194/hess-2020-468
Preprint. Discussion started: 26 October 2020


Hydrology and Earth System Sciences
Discussions

3.2.2 Multifractal intersection theorem

We would like now to illustrate and emphasise why it is so much indispensable to take into account the multiscale space variability of both the rainfall and the NBS distribution. For instance, both "hot spots" (extremes) of the rainfall and NBS are scarce and therefore could rarely coincide, i.e., rainfall spikes may fall more often elsewhere than on NBS. Similar questions can occur for less extreme events. The effective NBS performance could be therefore biased with respect to their potential performance due to this problem of intersection between rainfall intensity and NBS. It reminds us of the so-called multifractal intersection theorem applied to the intersection of a rainfall with extreme space variability and a rain gauge network that provides quantitative estimates of this intersection (Tchiguirinskaia et al., 2004). Figure 7, adapted from this paper, schematically represents the intersection at a given time of a (multifractal) rainfall, displaying quite variable pixel intensities ranging from light blue to dark brown (e.g., from 1 to 100 mm h^{-1}), with a heterogeneous rain gauge network (light brown pixels). The resulting measured rainfall field M is simply the product of the rainfall intensities R by the gauge characteristic function N (=1 if there is a gauge in this pixel, 0 otherwise). The intersection theorem states that for fractal objects, like for the usual (Euclidean) geometric ones, the codimension – i.e. the complement $c_M = d - D_M$ of the dimension D_M to the embedding space dimension d – of the measured field above a given intensity threshold is the sum of the codimensions of the network ($c_N = d - D_N$) and of the "real" field ($c_R = d - D_R$) above the same intensity threshold:

$$c_M = c_N + c_R \Leftrightarrow D_M = D_N + D_R - d \quad (4)$$

For instance, the intersection in a plane ($d = 2$) of two straight lines ($D_N = D_R = 1$; $c_N = c_R = 1$) corresponds to a point ($c_M = 2$, $D_M = 0$). Of particular interest is the case where the intersection is so scarce that its codimension c_M is larger than the embedding dimension d, i.e. has a negative dimension D_M (Schertzer and Lovejoy, 1987). Due to Eq. (4), the codimension of the network c_N is thus the critical dimension of the (real) field under which the rainfall intensity is rarely measured by the network:

$$c_M > \mathrm{d} \Leftrightarrow D_M < 0 \Leftrightarrow D_R < c_N = d - D_N \quad (5)$$

More precisely, the smaller D_R is with respect to c_N, the rarer the real field R is measured. Let us mention that Paz et al., (2020) used this intersection theorem to determine when the adjustment of radar data by a rain gauge network becomes misleading instead of improving the data.

The assessment of the performance of an NBS network cannot be reduced to the binary question of presence or not of an NBS, like done for a rain gauge of a network. However, we can immediately state they will be more and more ineffective for rainfall intensity whose fractal dimension is more and more below the codimension c_N of the network. This is already an important information that can be used to design NBS and their networks. This also explains why we estimated in the previous subsection the fractal (co-) dimension of the NBS network, as well as to compare in section 4.3 simulations resulting from spatially uniform rainfalls ($D_R = d$, $c_R = 0$) and spatially heterogeneous rainfalls ($D_R < d$, $c_R > 0$).

https://doi.org/10.5194/hess-2020-468
Preprint. Discussion started: 26 October 2020


Hydrology and Earth System Sciences
Discussions

3.3 Modelling experiments

The overall target of the study is to investigate whether the spatial variability of rainfall and the spatial arrangement of NBS have an impact on the hydrological responses of NBS scenarios at the urban catchment scale. For this purpose, three sets of modelling experiments were prepared, and two indexes (PE_{Qp}, percentage error on peak flow; PE_V, percentage error on total runoff volume) were used for quantifying the uncertainty associated to rainfall and NBS spatial distribution in the hydrological response of the catchment. Figure 8 presents the flow chart of the three sets of modelling experiments. In addition, the corresponding descriptions are presented as follows:

The first set is used to investigate the impact of spatial variability of rainfall on the hydrological responses of NBS scenarios. In this first set, we employed the following scenarios: baseline, PP1, RG1, GR1, and Combined1. These five scenarios were simulated under the distributed and uniform rainfall events. Then, we compute the ratio on peak flow (Eq. (6)), and the PE_{Qp} and PE_V (Eq. (7) and Eq. (8)) indexes for each scenario under two different kinds of rainfall.

The second set is used to analyse the impact of the spatial distribution of NBS on the hydrological responses of NBS scenarios. In this experiment, we compared the two groups of NBS scenarios mentioned in the Section 3.2 (GR1 vs GR2 for instance). The eight scenarios were only simulated with the uniform rainfall in order to avoid the impact of spatial variability of rainfall and to focus on the uncertainty associated with the spatial arrangement of NBS.

The third set is used to analyse the intersection impact of spatial variability of rainfall and the spatial distribution of NBS on the hydrological responses of the catchment. In this experiment, the eight mentioned NBS scenarios were simulated under the distributed and uniform rainfall, respectively. Then, the PE_{Qp} and PE_V of each NBS scenario were computed by comparing the results obtained for the two different kinds of rainfall events (distributed and uniform). Finally, we compare the difference of PE_{Qp} and the difference of PE_V between the NBS scenarios characterized by the same solutions/measures.

The peak flow ratio and the two indexes are especially calculated for the sum of four highlighted conduits connected to the catchment outlet (the right side of Fig. 2) with Eq. (6), (7) and (8):

$$Ratio = \frac{Q_{p_1}}{Q_{p_2}} \tag{6}$$

$$PE_{Q_p}(\%) = \frac{|Q_{p_1} - Q_{P_2}|}{Qp_1} \times 100 \tag{7}$$

$$PE_V(\%) = \frac{|V_1 - V_2|}{V_1} \times 100 \tag{8}$$

where Q_{p_1} and Q_{P_2} refer to the peak flow of scenarios under distributed rainfall and uniform rainfall respectively for the first and third modelling experiment. For the second experiment, they represent the peak flow of the first set of NBS scenarios and the second set of NBS scenarios, respectively. Correspondingly, for the first and third modelling experiments, V_1 and V_2 refer to the total runoff volume of scenarios under the distributed and uniform rainfall respectively. For the second modelling experiment, they represent the total runoff volume of the first set of NBS scenarios and the second set of NBS scenarios, respectively.

https://doi.org/10.5194/hess-2020-468
Preprint. Discussion started: 26 October 2020


Hydrology and Earth System Sciences
Discussions

3.4 Validation

Before the simulation of NBS scenarios, Multi-Hydro was validated with the water levels of the storage basin by applying the baseline scenario under the three distributed rainfall events. The simulations were then repeated with the three uniform rainfall events, respectively. The model performance was evaluated through two indicators: Nash-Sutcliffe Efficiency (*NSE*) and percentage error (*PE*). The Nash-Sutcliffe Efficiency (*NSE* ≤1) is an indicator generally used to verify the quality of the hydrological model simulation results, described as follows:

$$NSE(S_i, O_i) = 1 - \frac{\sum_{i=1}^{n}(O_i - S_i)^2}{\sum_{i=1}^{n}(O_i - \overline{O})^2} \quad (9)$$

where S_i refers to simulated values, O_i refers to observed values, and $\overline{O}$ represents the average of the observed values. The *NSE* closer to 1 indicates that the model is more reliable, whereas *NSE* closer to 0 indicates that the simulation does not better than that of the average observed value $\overline{O}$, which means the simulation performance is rather poor. If *NSE* is far less than 0, it means the simulation is even less performing than $\overline{O}$.

The percentage error (*PE*) represents the difference between observed values and simulation values, which reflects the reliability of the simulation values.

$$PE(S_i, O_i) = \frac{\sum_{i=1}^{n}|O_i - S_i|}{\sum_{i=1}^{n} O_i} \times 100\% \quad (10)$$

With respect to the observed and simulated water levels in the baseline scenario, the *NSE* coefficients and *PE* values are summarized in Table 4. For the three distributed rainfall events (Fig. 9), the *NSE* are larger than 0.9, and *PE* are lower than 5 %. For the uniform rainfall event of EV2, the model represents the water levels with *NSE* equal to 0.95, and *PE* equal to 1.96 %: only a slight overestimation of the observed water levels is observed between hours 4 to 7. For the uniform rainfall of EV1 and EV3, the temporal evolutions of simulated water levels slightly underestimate the observed ones, with *NSE* around 0.8, as well as *PE* around 7 %. Regarding the temporal evolutions of simulated water levels under the distributed rainfall of EV1 and EV3, they are more consistent with the observed ones. The reason is that the rainfall intensities of the distributed rainfall are generally higher than those of the uniform rainfall at the storage basin location. Namely, in uniform rainfall events, the accumulated water levels in the storage basin are less than that of in distributed rainfall events. Overall, the distributed rainfall gives slightly better results, and the simulated water levels using uniform rainfall also match sufficiently well the observed ones to validate the Multi-Hydro implementation in the Guyancourt catchment.

Hence, the Multi-Hydro is suitable and sufficiently reliable to investigate the impacts of spatial variability, either of rainfall and/or of NBS arrangements, on the hydrological responses under various NBS scenarios.

https://doi.org/10.5194/hess-2020-468
Preprint. Discussion started: 26 October 2020


Hydrology and Earth System Sciences
Discussions

4 Results and discussion

4.1 Impacts of spatial variability of rainfall

The impact of spatial variability of rainfall on the hydrological responses of each NBS scenario over the whole catchment was evaluated integrally in terms of the sum of flow in four conduits (highlighted in the right side of Fig. 2). These four conduits are chosen because they collect the runoff from the whole catchment and finally merge into the storage unit representing the outlet of the drainage system. To be more specific, the PE_{Qp} and the PE_V computed for the first set of modelling experiments (described in Sect. 3.3) are presented in the following section.

4.1.1 Baseline scenario

Before going on, it is important to evaluate the 'baseline' scenario under both distributed and uniform rainfalls, by using the simulations already performed to validate the Multi-Hydro implementation in the Guyancourt catchment. As shown in the hydrographs (Fig. 10a, b, c), the higher peak flow was generated by the distributed rainfall in EV1 and EV2. Hence, the peak flow ratio computed by comparing distributed rainfall and uniform rainfall is larger than 1 (see the first column of Fig. 12c), but this ratio is around 0.9 in EV3. The reason is that during the largest rainfall peak of EV1 and EV2, the rainfall intensity of all radar pixels in distributed rainfall is higher than those of uniform rainfall. While in EV3, the rainfall intensity of around 30 % radar pixels in uniform rainfall is about 28 mm h^{-1} higher than that of the distributed rainfall.

As shown in Fig. 12a, the PE_{Qp} of baseline scenario in EV1, EV2 and EV3 is about 9 %, 16 %, and 11 %, respectively. According to the *SD* of the rainfall intensity at the largest rainfall peak of each event (Table 1), the spatial variability of the rainfall intensity of EV2 is more pronounced than that of EV1 and EV3. Accordingly, the PE_{Qp} of baseline scenario in EV2 is the highest. Regarding the total runoff volume (Fig. 12b), the PE_V of the baseline scenario for the three rainfall events range from 1 % to 3.7 %. Contrary to the PE_{Qp}, the PE_V of the baseline scenario is not correlated to the *SD* of the total rainfall depth. For the baseline scenario, it is noticed that the PE_{Qp} is more pronounced than PE_V for all rainfall events. These results can be explained by the fact that the spatial variability of rainfall intensity at the largest rainfall peak is strong in all three rainfall events, while the spatial variability of the total rainfall depth is relatively uniform.

4.1.2 NBS scenarios

Figure 11 presents the simulated flow of the first set of NBS scenarios under the three distributed rainfall and three uniform rainfall events. The results are generally consistent with the results of the baseline scenario. Indeed, as shown in Fig. 12c, the peak flow ratios between distributed rainfall and uniform rainfall simulations for the four NBS scenarios are larger than 1 for EV1 and EV2, and around 0.8 for EV3 for the reason mentioned in the previous section.

As shown in Fig. 12a, the results of PE_{Qp} for PP1, RG1, and Combined1 scenarios are generally in agreement with the baseline scenario: PE_{Qp} is the lowest for EV1, and the highest for EV2. For these three NBS scenarios, PE_{Qp} range from about 8 % to 15 % for the three rainfall events. The relationship between the *SD* of the rainfall intensity at the largest rainfall peak and the

https://doi.org/10.5194/hess-2020-468
Preprint. Discussion started: 26 October 2020


Hydrology and Earth System Sciences
Discussions

PE_{Qp} of each NBS scenario (Fig. 13a) show that PE_{Qp} (the uncertainty related to the peak flow) computed for PP1, RG1, and Combined1 scenarios increase simultaneously with the increase of the *SD* of the rainfall intensity. The results computed for GR1 scenario do not depict the same tendency: PE_{Qp} computed for EV3 is higher than those computed for the two other events. The reason is related to various factors. Namely, it may be affected by the intersection effects of the spatial variability of rainfall and the spatial arrangement of green roofs in the catchment. As already mentioned, in EV3, the rainfall intensity of 30 % radar pixels in uniform rainfall is about 28 mm h^{-1} higher than that of the distributed rainfall. Coincidentally, in the GR1 scenario, the green roofs are mainly implemented on the locations with low distributed rainfall intensities. As demonstrated by many previous studies (Qin et al., 2013; Palla and Gnecco, 2015; Ercolani et al., 2018), GR are usually more effective for low rainfall intensity. In the case of the GR1 scenario under the distributed rainfall of EV3, GR measures stored more runoff than in the uniform rainfall during the main rainfall peak. This enlarges the variability of the hydrological response in terms of peak flow.

Regarding the percentage errors on total runoff volume, it is noticed that the computed PE_V are lower than 6 % for all NBS scenarios under the three rainfall events, especially in EV3, where they are lower than 2 %. This demonstrates that the resulting uncertainty on the total runoff volume is little influenced by the spatial variability of the rainfall. The reason is that the spatial variability of total rainfall depth is less pronounced with respect to the spatial variability of the rainfall intensity, and also there is no highly localized storm cell in studied events. As illustrated in Fig. 13b, the relationship between the *SD* of total rainfall depth and the PE_V of NBS scenarios is nonlinear. This can be explained by the fact that the three rainfall events are relatively long, and the hydrological performances of NBS are gradually changed during the event (e.g. they can efficiently infiltrate or store water at the beginning, and be saturated after a long rainfall period). Comparing the PE_V of each NBS scenario for all three rainfall events (Fig. 12b), those computed for GR1 and Combined1 appear to be the highest for EV2. It could be also related to the intersection effects of spatial location of GR measures and the spatial variability of rainfall. Indeed, these GR measures (considered in the GR1 and Combined1 scenarios) are mainly located in the north side of the catchment. In this area, the first distributed precipitation of EV2 (1-3.5 h), is relatively weak and variable (i.e., there is no rainfall or the rainfall with very low intensity in some localization pixels). Furthermore, as the initial moisture condition of GR measures are considered as unsaturated in both distributed and uniform rainfall, the GR measures are more efficient at the beginning of the distributed rainfall than in the uniform rainfall, and finally enlarge the uncertainty associated with precipitation variability (i.e., the corresponding PE_V). More discussion about the intersection effects is presented in Section 4.3.

4.2 Impacts of the spatial distribution of NBS

In order to analyze the impacts of the spatial distribution of NBS on the hydrological responses of NBS scenarios, the results of the second set of modelling experiment (described in Section 3.3) are presented as follows. As shown in Fig. 14a, the PE_{Qp} of all NBS scenarios are lower than 5 %, and the PE_V of all NBS scenarios are lower than 7 %, which indicates that the hydrological responses of NBS scenarios are little affected by the spatial distribution of NBS in the catchment. This result is generally consistent with the observation of Versini et al., (2016), who pointed out that the impact of the spatial distribution

https://doi.org/10.5194/hess-2020-468
Preprint. Discussion started: 26 October 2020


Hydrology and Earth System Sciences
Discussions

of green roofs on the catchment response is minimal. However, comparing the PE_{Qp} of each NBS scenario, those computes for PP and GR scenarios range from about 2 % to 5 %, which are slightly higher than those related to other scenarios, especially for EV1 and EV3. The reason can be explained by two factors: (i) the infiltration or detention capacity of PP and GR measures are less effective for rainfall characterized by strong intensity and long duration (Qin et al., 2013; Palla and Gnecco, 2015), whereas the RG measures are artificial depressed green areas (simulated with a 0.3 m substrate) with higher retention capacity (Dussaillant et al., 2004); (ii) the differences of D_F (large scale; i.e., the second regime) between PP1 and PP2 scenarios as well as between GR1 and GR2 scenarios are larger than that of the other NBS scenarios (Table 3). Figure 15a shows the difference of D_F between the same types of NBS scenarios is proportional to the corresponding PE_{Qp}. It is found that the larger the difference of D_F, the higher the PE_{Qp} is. Regarding the PE_V of NBS scenarios for the three uniform rainfall events (Fig. 14b), those comparing PP1 and PP2 scenarios (which ranges from about 4 % to 7 % for the three rainfall events, especially higher for the two strong and long events) are slightly higher than those related to the other scenarios. Because porous pavements are infiltration-based measures (they do not retain water for a limited period), their performances are more related to the heterogeneity of their performed location. Namely, some PP measures implemented in drained areas may suffer more from surface runoff, are therefore more easily saturated (see Fig. 5 for a comparison of the spatial arrangement of PP measures for two PP scenarios). As shown in Fig. 15b, the difference of D_F between the same types of NBS scenarios has a moderate positive correlation (r =0.61) with the corresponding PE_V. Our study hypothesizes that this rather weak correlation is related to the complexity of rainfall with several peaks and dry periods, the retention/infiltration capacity of NBS changes with the rainfall intermittency.

4.3 Intersection effects of spatial variability of rainfall and spatial arrangement of NBS

In the following, we present the results of the third modelling experiment set described in Sect. 3.3. The aim is to analyse the potential intersection effects of spatial variability of rainfall and spatial distribution of NBS on the hydrological responses of NBS scenarios.

The resulting uncertainty on the peak flow and total runoff volume (PE_{Qp} and PE_V) of the third set of modelling experiments are shown in Fig. 16. Firstly, we found that the spatial variability of rainfall has a certain extent impact on the peak flow of each scenario, with the PE_{Qp} ranging from about 8 % to 17 %. With the exception of GR1, all the NBS scenarios have a similar tendency: the PE_{Qp} are the lowest for the first event, and the highest for the second one. Namely, for most of NBS scenarios, the PE_{Qp} (uncertainty on peak flow) increases with the increase of the spatial variability of rainfall intensity. As shown in Fig. 16a, comparing the PE_{Qp} between scenarios of PP1 and PP2, RG1 and RG2, as well as Combined1 and Combined2 for the three rainfall events, the maximum difference is less than 3 %. However, comparing the PE_{Qp} between GR1 and GR2, the difference is larger, especially in EV3 (> 5 %). For the GR1 scenario, PE_{Qp} range from about 8 % to 17 % in all three rainfall events, and those of GR2 range from about 10 % to 15 %. Furthermore, for GR1, the largest PE_{Qp} is in EV3, but for GR2, the largest PE_{Qp} is computed for EV2. The difference of PE_{Qp} between GR1 and GR2 scenarios demonstrated that the spatial variability of rainfall and the spatial arrangement of GR measures have some intersection effects on the peak flow of GR

https://doi.org/10.5194/hess-2020-468
Preprint. Discussion started: 26 October 2020


Hydrology and Earth System Sciences
Discussions

scenarios. However, it is not evident for the other NBS scenarios. One of the reasons has been discussed in Sect. 4.1.2: in the GR1 scenario, GR measures are mainly implemented in the north part of the catchment, which coincidently received lower rainfall (distributed EV3); namely, the"hot spots" of the rainfall field were scarcely intersected by the GR measures due to their low fractal dimension. Another possible reason is GR has the lowest storage capacity in the studied NBS, as well as the studied rainfall events are not intense enough to saturate the other types of NBS.

Concerning the intersection impact on total runoff volume of NBS scenarios, the variations of PE_V among most of NBS scenarios pairs (PP1 and PP2, GR1 and GR2, as well as Combined1 and Combined2) are significantly different for the three rainfall events. The maximum discrepancy (higher than 5 %) is noticed between Combined1 and Combined2 in EV3, because the two combined scenarios mixed three types of NBS with different retention capacity, and the total rainfall depth is more variable for EV3. Conversely, the difference of PE_V between RG1 and RG2 is relatively small, which is less than 1 %. The reason can be explained by the large retention capacity of RG measures, which has been mentioned in Sec.4.2.

Overall, the results demonstrate that the spatial variability of rainfall and the spatial arrangement of NBS can generate uncertainties on peak flow and total runoff volume estimations if they are not considered properly. In this specific case, they are more significant for GR scenarios, while less evident for RG scenarios.

5 Conclusions

This paper focused on the variability of the hydrological responses of NBS scenarios resulting from the multiscale spatial heterogeneity of both the rainfall and the NBS distribution. We pointed out how the "multifractal intersection theorem" can quantify how often they intersect, which conditions the NBS performance. The high-resolution distributed rainfall data from the ENPC X-band radar depict the spatially variable rainfall fields. The fully-distributed and physically-based hydrological model (Multi-Hydro) takes into account the heterogeneity of an urban environment down to the 10 m scale, including the spatial arrangement of NBS and spatial distribution of rainfall. The principal findings are summarized as follows:

1. The spatial variability of rainfall has a significant impact on the peak flow of NBS scenarios for the three studied rainfall events. For instance, it makes the maximum PE_{Qp} increase up to 17 % in GR1 scenario. Furthermore, the spatial variability of the rainfall intensity at the largest rainfall peak is almost linearly related to the PE_{Qp} computed for all NBS scenarios (except for GR1): the more variable are the rainfall intensities, the higher are the PE_{Qp}. However, the resulting PE_V computed for all NBS scenarios show that the spatial variability of rainfall has much lower impact on the uncertainty related to total runoff volume: the average PE_V being of the order of 2.3 % only.
2. The impact of spatial arrangement of NBS on hydrological responses of the catchment is less obvious. For all the NBS scenarios, PE_{Qp} and PE_V are lower than 5 % and 7 %, respectively. However, we found that the difference of D_F between the same types of NBS scenarios has a fairly strong positive correlation to the related PE_{Qp}. Therefore, we suggest to implement NBS by optimizing D_F over the whole catchment to be the highest possible. Furthermore, mixing different NBS in the catchment, as presented in the two combined scenarios, can also efficiently reduce the uncertainty associated with the spatial arrangement of NBS.

https://doi.org/10.5194/hess-2020-468
Preprint. Discussion started: 26 October 2020


Hydrology and Earth System Sciences
Discussions

3. The fractal dimension D_F appears as a useful tool to quantify the spatial heterogeneity of NBS across a range of scales. The D_F of each NBS scenario is associated with the urbanization level of the catchment, which confirms that the level of implementation of NBS is reasonable to match the catchment conditions. The fractal dimension combined with the fully-distributed model is an innovative approach that is easily transportable to other catchments.
4. The spatial distribution of rainfall and the spatial arrangement of NBS have intersection effects on the hydrological responses of NBS scenarios, especially significant for the peak flow of GR scenarios (with a maximum difference between the scenario of GR1 and GR2 reaching about 5 % on peak flow). The intersection effects on the total runoff volume of each NBS scenario is quite variable because the chosen NBS present some limitations in terms of infiltration or detention capacity during a long rainfall event with high intermittency. However, the RG scenarios appear to be less affected by the intersection effects, with a difference lower than 3 % on peak flow and lower than 1 % on total runoff volume.
5. The fully-distributed model takes into account the spatial rainfall variability and the spatial distribution of NBS at very small scale, which presents the uncertainty of hydrological performances of NBS scenarios (e.g. peak flow and total runoff volume) is related to these two factors. Whereas the lumped and semi-distributed models are not able to consider these heterogeneities, and the level of spatial resolution incorporate in this type of models may result in some critical heterogeneous information be missing that can influence model predictions.

In our specific case, the GR scenarios are more sensitive to the spatial variability of rainfall and the spatial arrangement of GR measures, while the performances of RG scenarios and combined scenarios are more stable under any condition. Apparently, these findings already give some incites to decision-makers on *Why* they need to prioritize given NBS within the urban planning process.

However, larger rainfall samples, including extreme rainfalls, will be needed to provide a better knowledge towards the somewhat universal solutions and to give an answer on *How* to prioritize these NBS. Under this perspective, the obtained results already demonstrated that new scale-independent indictors, like the fractal dimension D_F applied in this study, will be essential for more profound quantitative evaluation of the diversity of combined impacts, including for other heterogeneous catchments.

Data availability. Datasets for this study are under preparation for public release by the Chair Hydrology for Resilience Cities. They can already be freely obtained via contact.hmco@enpc.fr.

Model availability. The version 2.1 of Multi-Hydro is registered by the (France) Program Protection Agency (IDDN FR 001 340017 000 SC 2015 0000 31235) and can be freely obtained via contact.hmco@enpc.fr.

Author contribution. Yangzi Qiu performed the modelling experiments, data analysis and wrote the paper with contributions from all co-authors. Ioulia Tchiguirinskaia, Daniel Schertzer, conceived and supervised the study. Yangzi Qiu and Pierre-Antoine Versini created and implemented various scenarios. Yangzi Qiu and Igor Paz prepared the input data for the model. All co-authors revised the manuscript.

Competing interests. The authors declare that they have no conflict of interest.

Acknowledgements. The first author greatly acknowledges the financial support by the China Scholarship Council. The first author furthermore highly acknowledges Abdellah ICHIBA for his precious help in taking over the Multi-Hydro model. All the authors acknowledge the Chair "Hydrology for Resilient Cities" (endowed by VEOLIA), for partial financial support and express gratitude to their colleagues from SIAVB and Veolia, particularly Bernard WILLINGER, for many stimulating discussions. The authors acknowledge the agglomeration community of Saint-Quentin-en-Yvelines for providing the data of the Guyancourt catchment; and express thanks to Aderson Dion ́sio Leite Neto for his help with numerical pre-processing of these data, as a part of his secondment at Ecole des Ponts ParisTech.

References

Ahiablame, L. and Shakya, R.: Modeling flood reduction effects of low impact development at a watershed scale, J. Environ. Manage., 171, 81–91, doi:10.1016/j.jenvman.2016.01.036, 2016.

Ahiablame, L. M., Engel, B. A. and Chaubey, I.: Effectiveness of low impact development practices in two urbanized watersheds: Retrofitting with rain barrel/cistern and porous pavement, J. Environ. Manage., 119, 151–161, doi:10.1016/j.jenvman.2013.01.019, 2013.

Alves de Souza, B., da Silva Rocha Paz, I., Ichiba, A., Willinger, B., Gires, A., Amorim, J.C.C., de Miranda Reis, M., Tisserand, B., Tchiguirinskaia, I. and Schertzer, D.: Multi-hydro hydrological modelling of a complex peri-urban catchment with storage basins comparing C-band and X-band radar rainfall data, Hydrol. Sci. J., 63, 1619–16352018, https://doi.org/10.1080/02626667.2018.1520390, 2018.

Berry, P. M., Elmqvist, T., Hartig, T. and Naumann, S.: EUROPEAN COMMISSION Directorate-General for Research and Innovation Directorate I-Climate Action and Resource Efficiency Unit I.3-Sustainable Management of Natural Resources, 2015.

Bloorchian, A.A., Ahiablame, L., Osouli, A., Zhou, J., 2016. Modeling BMP and Vegetative Cover Performance for Highway Stormwater Runoff Reduction, in: Procedia Engineering. pp. 274–280. https://doi.org/10.1016/j.proeng.2016.04.074.

Bozovic, R., Maksimovic, C., Mijic, A., Smith, K.M., Suter, I., van Reeuwijk, M., 2017. Blue Green Solutions: A Systems Approach to Sustainable, Resilient and Cost-Efficient Urban Development 52. https://doi.org/10.13140/RG.2.2.30628.07046.

https://doi.org/10.5194/hess-2020-468
Preprint. Discussion started: 26 October 2020


Hydrology and Earth System Sciences
Discussions

Burszta-Adamiak, E. and Mrowiec, M.: Modelling of Green roofs' hydrologic performance using EPA's SWMM, Water Sci. Technol., 68(1), 36–42, doi:10.2166/wst.2013.219, 2013.

Cipolla, S. S., Maglionico, M. and Stojkov, I.: A long-term hydrological modelling of an extensive green roof by means of SWMM, Ecol. Eng., 95, 876–887, doi:10.1016/j.ecoleng.2016.07.009, 2016.

Cohen-Shacham, E., Walters, G., Janzen, C. and Maginnis, S.: Nature-based solutions to address global societal challenges, IUCN, Gland, Switzerland, 2016.

Carter, T. L. and Rasmussen, T. C.: Hydrologic Behavior of Vegetated Roofs, J. Am. Water Resour. Assoc., 42(5), 1261–1274, doi:10.1111/j.1752-1688.2006.tb05611.x, 2007.

Dussaillant, A. R., Wu, C. H. and Potter, K. W.: Richards Equation Model of a Rain Garden, J. Hydrol. Eng., 9(3), 219–225, doi:10.1061/(asce)1084-0699(2004)9:3(219), 2004.

El Tabach, E., Tchiguirinskaia, I., Mahmood, O. and Schertzer, D.: Multi-Hydro: a spatially distributed numerical model to assess and manage runoff processes in peri- urban watersheds. Poster session presentation at the Final Conference of the COST Action C22, Road map towards a flood resilient urban environment, Paris, France, 2009.

Ercolani, G., Chiaradia, E. A., Gandolfi, C., Castelli, F. and Masseroni, D.: Evaluating performances of green roofs for stormwater runoff mitigation in a high flood risk urban catchment, J. Hydrol., 566(September), 830–845, doi:10.1016/j.jhydrol.2018.09.050, 2018.

Fry, T. J. and Maxwell, R. M.: Evaluation of distributed BMPs in an urban watershed—High resolution modeling for stormwater management, Hydrol. Process., 31(15), 2700–2712, doi:10.1002/hyp.11177, 2017.

Gilroy, K. L. and McCuen, R. H.: Spatio-temporal effects of low impact development practices, J. Hydrol., 367(3–4), 228–236, doi:10.1016/j.jhydrol.2009.01.008, 2009.

Gires, A., Tchiguirinskaia, I., Schertzer, D. and Lovejoy, S.: Multifractal analysis of a semi-distributed urban hydrological model, Urban Water J., 10(3), 195–208, doi:10.1080/1573062X.2012.716447, 2013.

Gires, A., Tchiguirinskaia, I., Schertzer, D., Ochoa-Rodriguez, S., Willems, P., Ichiba, A., Wang, L. P., Pina, R., Van Assel, J., Bruni, G., Murla Tuyls, D. and Ten Veldhuis, M. C.: Fractal analysis of urban catchments and their representation in semi-distributed models: Imperviousness and sewer system, Hydrol. Earth Syst. Sci., 21(5), 2361–2375, doi:10.5194/hess-21-2361-2017, 2017.

Gires, A., Abbes, J.-B., da Silva Rocha Paz, I., Tchiguirinskaia, I. and Schertzer, D.: Multifractal characterisation of a simulated surface flow: a case study with multi-hydro in Jouy-en-Josas, France, Journal of Hydrology, 558, 483–495. doi:10.1016/j.jhydrol.2018.01.062, 2018.

Hoang, T. Prise en compte des fluctuations spatio-temporelles pluies-débits pour une meilleure gestion de la ressource en eau et une meilleure évaluation des risques. Ph.D. Thesis, Earth Sciences, Université Paris-Est, Champs-sur-Marne, France, 2011.

Hamidi, A., Farnham, D. J. and Khanbilvardi, R.: Uncertainty analysis of urban sewer system using spatial simulation of radar rainfall fields: New York City case study, Stoch. Environ. Res. Risk Assess., 32(8), 2293–2308, doi:10.1007/s00477-018-1563-8, 2018.

https://doi.org/10.5194/hess-2020-468
Preprint. Discussion started: 26 October 2020

Giangola-Murzyn, A. : Modélisation et paramétrisation hydrologique de la ville, résilience aux inondations, Ph.D. thesis, Ecole des Ponts ParisTech, Université Paris-Est, France, 260 pp., 2013.

Giangola-Murzyn, A., Richard, J., Gires, A., Fitton, G., Tchiguirinskaia, I. and Schertzer, D.: Multi-Hydro Notice and Tutorial. Laboratoire Eau Environnement et Systèmes Urbains, École des Ponts ParisTech. Université Paris-Est, France, 44 pp., 2014.

Guo, X., Du, P., Zhao, D. and Li, M.: Modelling low impact development in watersheds using the storm water management model, Urban Water J., 16(2), 146–155, doi:10.1080/1573062X.2019.1637440, 2019.

Hentschel H G E, Procaccia I. : The infinite number of generalized dimensions of fractals and strange attractors[J]. Physica D: Nonlinear Phenomena, 8(3): 435-444. doi:10.1016/0167-2789(83)90235-X, 1983.

Her, Y., Jeong, J., Arnold, J., Gosselink, L., Glick, R. and Jaber, F.: A new framework for modeling decentralized low impact developments using Soil and Water Assessment Tool, Environ. Model. Softw., 96, 305–322, doi:10.1016/j.envsoft.2017.06.005, 2017.

Holman-Dodds, J. K., Bradley, A. A. and Potter, K. W.: Evaluation of hydrologic benefits of infiltration based urban storm water management, J. Am. Water Resour. Assoc., 39(1), 205–215, doi:10.1111/j.1752-1688.2003.tb01572.x, 2003.

Hu, M., Sayama, T., Zhang, X., Tanaka, K., Takara, K. and Yang, H.: Evaluation of low impact development approach for mitigating flood inundation at a watershed scale in China, J. Environ. Manage., 193, 430–438, doi:10.1016/j.jenvman.2017.02.020, 2017.

Hakimdavar, R., Culligan, P. J., Finazzi, M., Barontini, S. and Ranzi, R.: Scale dynamics of extensive green roofs: Quantifying the effect of drainage area and rainfall characteristics on observed and modeled green roof hydrologic performance, Ecol. Eng., 73, 494–508, doi:10.1016/j.ecoleng.2014.09.080, 2014.

Ichiba, A. X-Band Radar Data and Predictive Management in Urban Hydrology. Ph.D. Thesis, Earth Sciences, Université Paris-Est, Champs-sur-Marne, France, 2016.

Ichiba, A., Gires, A., Tchiguirinskaia, I., Schertzer, D., Bompard, P. and Veldhuis, M. C. Ten: Scale effect challenges in urban hydrology highlighted with a distributed hydrological model, Hydrol. Earth Syst. Sci., 22(1), 331–350, doi:10.5194/hess-22-331-2018, 2018.

Jia, H., Yao, H., Tang, Y., Yu, S. L., Field, R. and Tafuri, A. N.: LID-BMPs planning for urban runoff control and the case study in China, J. Environ. Manage., 149, 65–76, doi:10.1016/j.jenvman.2014.10.003, 2015.

Institut National de la Statistique et des Etudes Economiques – INSEE: Dossier complet – Commune de Guyancourt (78297). Available online: https://www.insee.fr/fr/statistiques/2011101?geo=COM-78297#chiffre-cle-5 (accessed on 29 February 2020).

James, W., Rossman, L. A. and James, W. R. C.: User's guide to SWMM5 based on original USEPA SWMM documentation., CHI, USA, 905, 2010.

Kelman, I.: Climate Change and the Sendai Framework for Disaster Risk Reduction, Int. J. Disaster Risk Sci., 6(2), 117–127, doi:10.1007/s13753-015-0046-5, 2015.

600 Kwak, D., Kim, H. and Han, M.: Runoff Control Potential for Design Types of Low Impact Development in Small Developing Area Using XPSWMM, in Procedia Engineering, vol. 154, pp. 1324–1332., 2016.

Lavallée, D., Lovejoy, S., Schertzer, D., Ladoy, P., 1993. Nonlinear variability and landscape topography: analysis and simulation. Fractals in geography, pp. 158–192.

Liu, Y., Ahiablame, L. M., Bralts, V. F. and Engel, B. A.: Enhancing a rainfall-runoff model to assess the impacts of BMPs
605 and LID practices on storm runoff, J. Environ. Manage., 147, 12–23, doi:10.1016/j.jenvman.2014.09.005, 2015.

Loukas, A., Llasat Botija, M. D. C. and Ulbrich, U.: Extreme events induced by weather and climate change: Evaluation, forecasting and proactive planning, Nat. Hazards Earth Syst. Sci., 10(9), 1895–1897, doi:10.5194/nhess-10-1895-2010, 2010.

Lovejoy, S. and Schertzer, D.: The weather and climate: Emergent laws and multifractal cascades., Cambridge University Press, UK, 491, 2013.

610 Lovejoy, S., Schertzer, D., Tsonis, A.A,: Functional Box-Counting and Multiple Elliptical Dimensions in Rain. Science 235, 1036–1038, doi: 10.1126/science.235.4792.1036, 1987.

Mandelbrot, B. B.: The fractal geometry of nature, vol. 173, Macmillan, 1983.

Massoudieh, A., Maghrebi, M., Kamrani, B., Nietch, C., Tryby, M., Aflaki, S. and Panguluri, S.: A flexible modeling framework for hydraulic and water quality performance assessment of stormwater green infrastructure, Environ. Model. Softw.,
615 92, 57–73, doi:10.1016/j.envsoft.2017.02.013, 2017.

Météo-France: Climat des Yvelines. Available online: https://www.meteofrance.com/accueil (accessed on 29 February 2020).

Miller, J. D. and Hutchins, M.: The impacts of urbanisation and climate change on urban flooding and urban water quality: A review of the evidence concerning the United Kingdom, J. Hydrol. Reg. Stud., 12(January), 345–362, doi:10.1016/j.ejrh.2017.06.006, 2017.

620 Newcomer, M. E., Gurdak, J. J., Sklar, L. S. and Nanus, L.: Urban recharge beneath low impact development and effects of climate variability and change, Water Resour. Res., 50(2), 1716–1734, doi:10.1002/2013WR014282, 2014.

Palla, A., Gnecco, I., Carbone, M., Garofalo, G., Lanza, L. G. and Piro, P.: Influence of stratigraphy and slope on the drainage capacity of permeable pavements: laboratory results, Urban Water J., 12(5), 394–403, doi:10.1080/1573062X.2014.900091, 2015.

625 Paz, I., Willinger, B., Gires, A., Ichiba, A., Monier, L., Zobrist, C., Tisserand, B., Tchiguirinskaia, I. and Schertzer, D.: Multifractal comparison of reflectivity and polarimetric rainfall data from C- and X-band radars and respective hydrological responses of a complex catchment model, Water (Switzerland), 10(3), doi:10.3390/w10030269, 2018.

Paz, I., Willinger, B., Gires, A., Alves de Souza, B., Monier, L., Cardinal, H., Tisserand, B., Tchiguirinskaia, I. and Schertzer, D.: Small-Scale Rainfall Variability Impacts Analyzed by Fully-Distributed Model Using C-Band and X-Band Radar Data,
630 Water (Switzerland), 11 (6), doi:10.3390/w11061273, 2019.

Paz, I.; Tchiguirinskaia, I., Schertzer, D.: Rain gauge networks' limitations and the implications to hydrological modelling highlighted with a X-band radar, Journal of Hydrology, 583, 124615, https://doi.org/10.1016/j.jhydrol.2020.124615, 2020.

Pyke, C., Warren, M. P., Johnson, T., LaGro, J., Scharfenberg, J., Groth, P., Freed, R., Schroeer, W. and Main, E.: Assessment of low impact development for managing stormwater with changing precipitation due to climate change, Landsc. Urban Plan., 103(2), 166–173, doi:10.1016/j.landurbplan.2011.07.006, 2011.

Qin, H. P, Li, Z. X and Fu, G.: The effects of low impact development on urban flooding under different rainfall characteristics, J. Environ. Manage., 129, 577–585, doi:10.1016/j.jenvman.2013.08.026, 2013.

Rossman, L. A.: Storm water management model user's manual, version 5.0, Cincinnati: National Risk Management Research Laboratory, Office of Research and Development, US Environmental Protection Agency, 276, 2010.

Richard, J., Giangola-Murzyn, A., Tchiguirinskaia, I. and Schertzer, D.: MH-ASSIMTOOL: An assimilation tool dedicated to a fully distributed model. Poster presented at International Conference on Flood Resilience. 5-7 September 2013. United Kingdom.

Schertzer, D. and Lovejoy, S., 1984. On the dimension of atmospheric motions. Turbulence and Chaotic phenomena in Fluids, pp. 505–512.

Schertzer, D. and Lovejoy, S., 1987. Physical modeling and analysis of rain and clouds by anisotropic scaling multiplicative processes. Journal of Geophysical Research: Atmospheres, 92(D8):9693–9714.

Schertzer, D. and Lovejoy, S., 1991. Nonlinear variability in geophysics.

Sun, Y.W., Li, Q. Y., Liu, L., Xu, C. D. and Liu, Z. P.: Hydrological simulation approaches for BMPs and LID practices in highly urbanized area and development of hydrological performance indicator system, Water Sci. Eng., 7(2), 143–154, doi:10.3882/j.issn.1674-2370.2014.02.003, 2014.

Stanić, F., Cui, Y. J., Delage, P., De Laure, E., Versini, P. A., Schertzer, D. and Tchiguirinskaia, I.: A device for the simultaneous determination of the water retention properties and the hydraulic conductivity function of an unsaturated coarse material; application to a green-roof volcanic substrate, Geotech. Test. J., 43(3), doi:10.1520/GTJ20170443, 2019.

Tchiguirinskaia, I., Schertzer, D., Hubert, P., Bendjoudi, H. and Lovejoy, S.: Multiscaling geophysics and sustainable development, IAHS Publ. Proc. Reports, 287, 113–136, 2004.

Velleux, M. L., England, J. F. and Julien, P. Y.: TREX: spatially distributed model to assess watershed contaminant transport and fate., Sci. Total Environ., 404(1), 113–128, doi:10.1016/j.scitotenv.2008.05.053, 2008.

Versini, P. A., Gires, A., Tchinguirinskaia, I. and Schertzer, D.: Toward an operational tool to simulate green roof hydrological impact at the basin scale: A new version of the distributed rainfall-runoff model Multi-Hydro, Water Sci. Technol., 74(8), 1845–1854, doi:10.2166/wst.2016.310, 2016.

Versini, P. A., Kotelnikova, N., Poulhes, A., Tchiguirinskaia, I., Schertzer, D. and Leurent, F.: A distributed modelling approach to assess the use of Blue and Green Infrastructures to fulfil stormwater management requirements, Landsc. Urban Plan., 173, 60–63, doi:10.1016/j.landurbplan.2018.02.001, 2018.

Versini P-A, Gires A, Tchiguirinskaia I, and Schertzer D.: Fractal analysis of green roof spatial implementation in European cities, Urban Forestry and amp; Urban Greening (2020), doi: https://doi.org/10.1016/j.ufug.2020.126629.

https://doi.org/10.5194/hess-2020-468
Preprint. Discussion started: 26 October 2020

Zahmatkesh, Z., Burian, S. J., Karamouz, M., Tavakol-Davani, H. and Goharian, E.: Low-Impact Development Practices to Mitigate Climate Change Effects on Urban Stormwater Runoff: Case Study of New York City, J. Irrig. Drain. Eng., 141(1), 4014043, doi:10.1061/(ASCE)IR.1943-4774.0000770, 2015.

Zhu, Z., Chen, Z., Chen, X. and Yu, G.: An assessment of the hydrologic effectiveness of low impact development (LID) practices for managing runoff with different objectives, J. Environ. Manage., 231(April 2018), 504–514, doi:10.1016/j.jenvman.2018.10.046, 2019.

https://doi.org/10.5194/hess-2020-468
Preprint. Discussion started: 26 October 2020

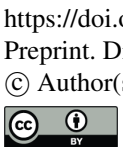

Hydrology and Earth System Sciences
Discussions
Open Access
EGU

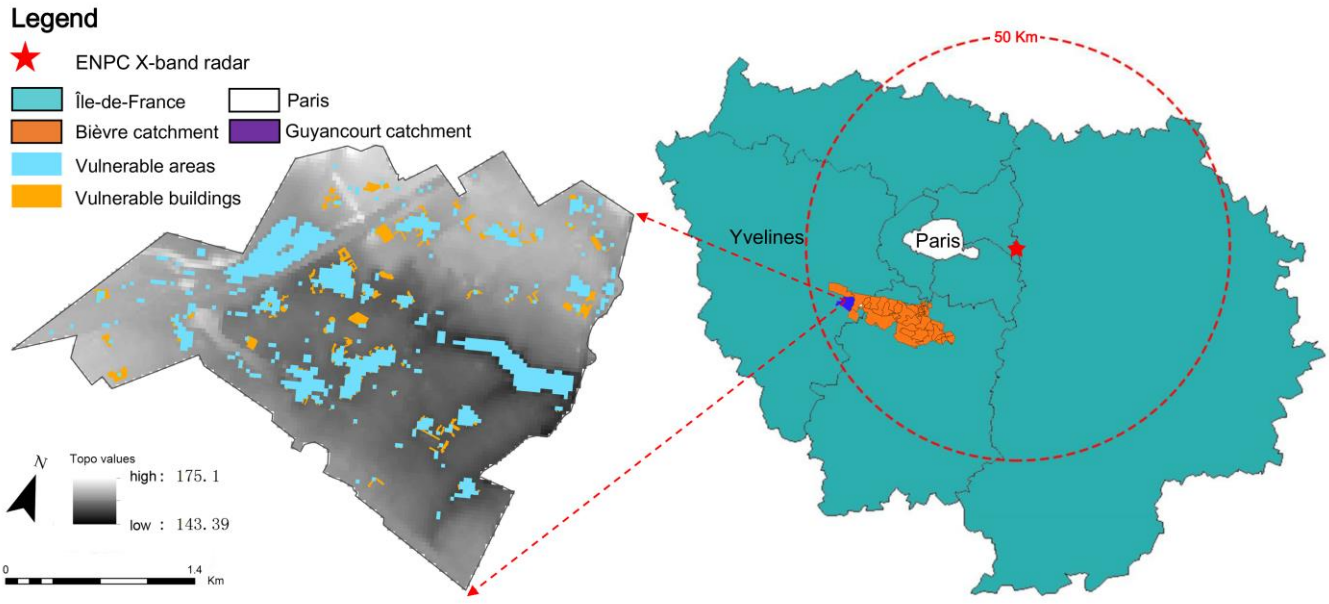

Figure 1: Location of the study site and the corresponding topography map, highlighting some vulnerable areas and buildings at risk of waterlogging in the Guyancourt catchment.

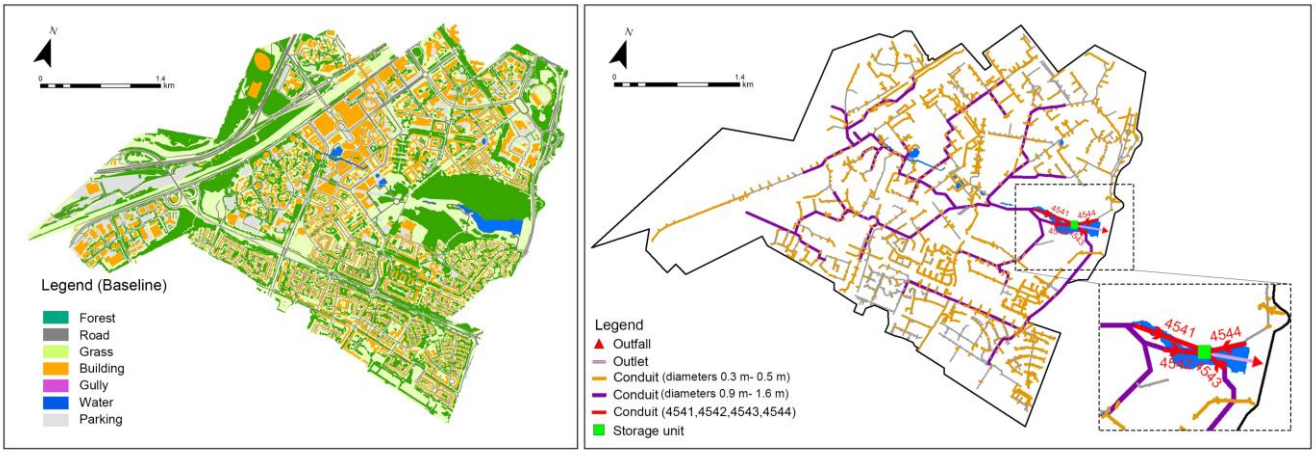

Figure 2: Left: land use map (baseline scenario). Right: drainage system with four conduits (4541, 4542, 4543, and 4544) highlighted.

https://doi.org/10.5194/hess-2020-468
Preprint. Discussion started: 26 October 2020

Hydrology and Earth System Sciences
Discussions

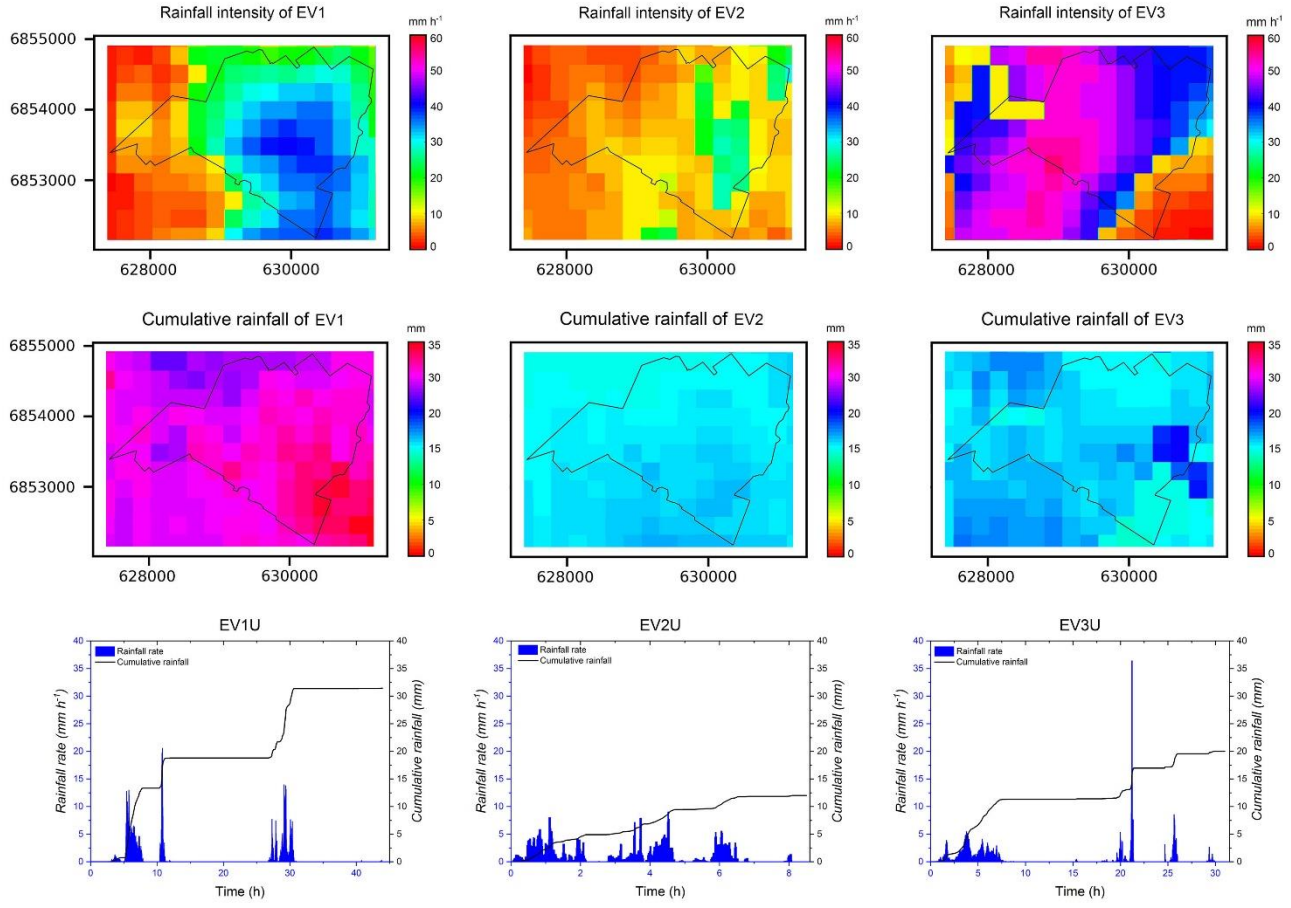

695

Figure 3: Top: The rainfall intensity at the largest rainfall peak (per radar pixel) over the Guyancourt catchment area for the three studied rainfall events. Middle: Cumulative rainfall depths (per radar pixel) over the Guyancourt catchment area for the three studied rainfall events. Bottom: Time evolution of rainfall rate (mm h^{-1}) and cumulative rainfall (mm) of the three uniform rainfall events over the whole catchment.

700

https://doi.org/10.5194/hess-2020-468
Preprint. Discussion started: 26 October 2020

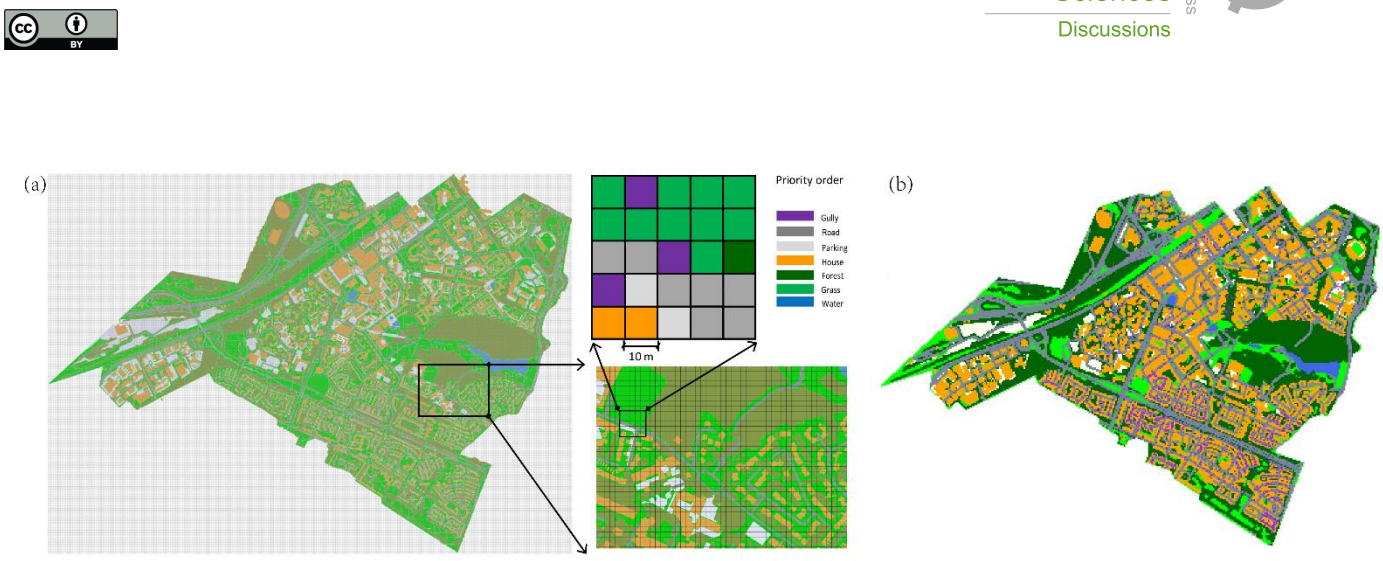

Figure 4: (a) Rasterization of the original land use data into 10 m with priority order, and (b) the rasterized land use data.

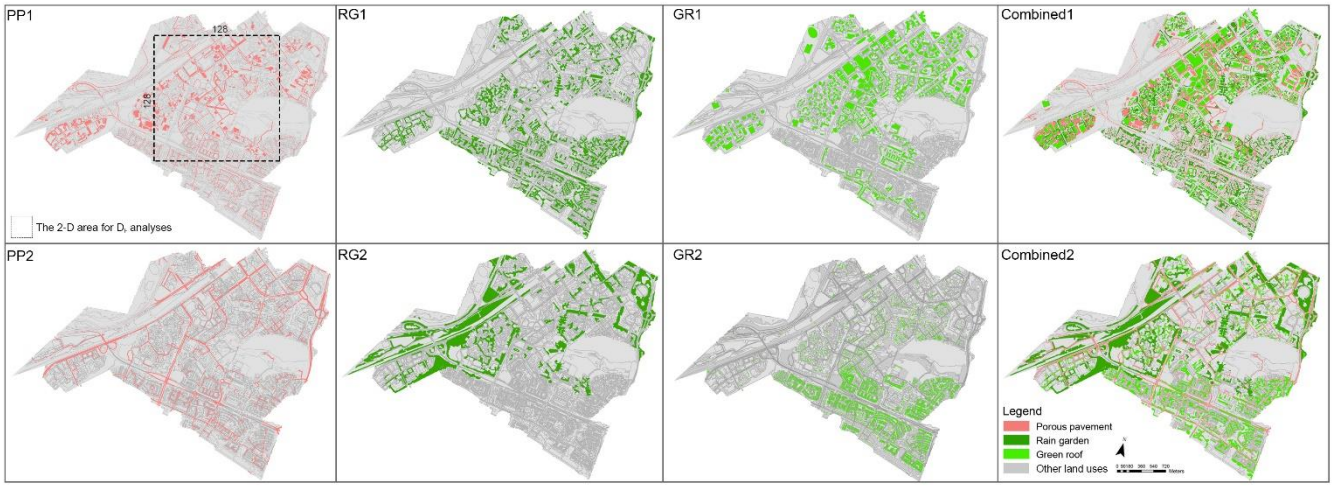

Figure 5: NBS scenarios including PP1, PP2, RG1, RG2, GR1, GR2, Combined1, and Combined2, the rectangular area that presented in the PP1 scenario is the example area for applying fractal analysis.

https://doi.org/10.5194/hess-2020-468
Preprint. Discussion started: 26 October 2020

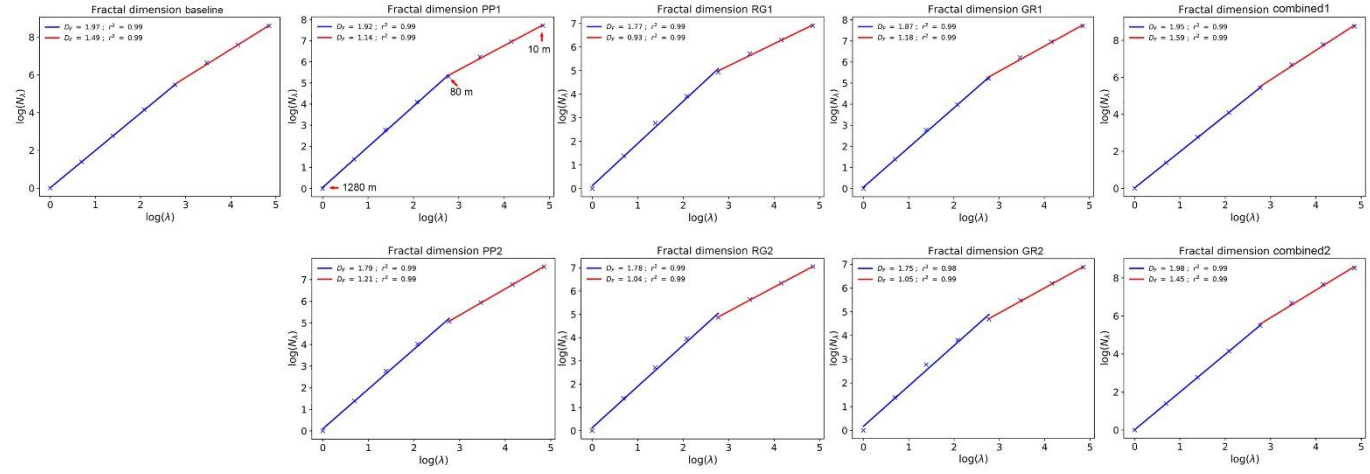

Figure 6: The fractal dimension of impervious surface of the baseline scenario and the fractal dimension of NBS in each NBS scenario.

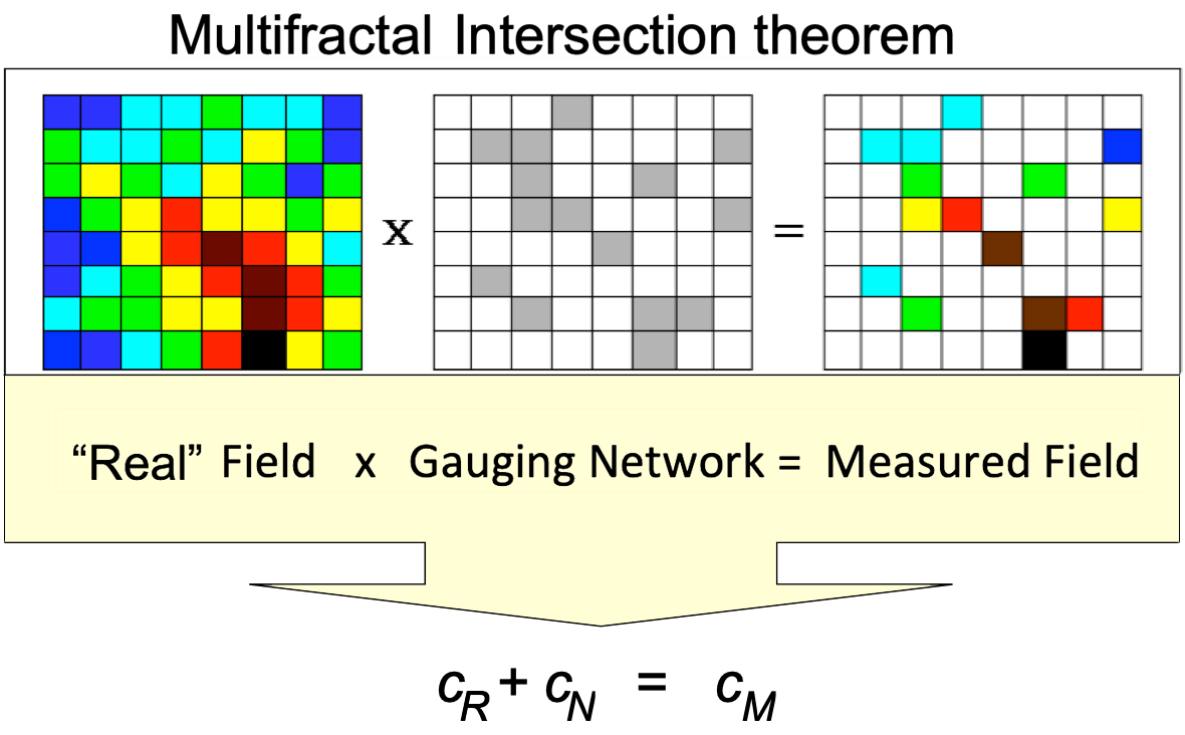

Figure 7: Schematic of the (multifractal) intersection theorem applied to the measured rainfall M by a rain gauge network N. The measured rainfall corresponds to the product of the "real" rainfall R by the gauge characteristic function (=1 if there is a gauge in this pixel, 0 otherwise) and the corresponding codimensions $c_R = d - D_R$ and $c_N = d - D_N$ add to yield the codimension of the measured rainfall $c_M = d - D_M$. d is the embedding space dimension, DR, DN and DM are the corresponding fractal dimensions (adapted from Tchiguirinskaia et al., 2004).

https://doi.org/10.5194/hess-2020-468
Preprint. Discussion started: 26 October 2020

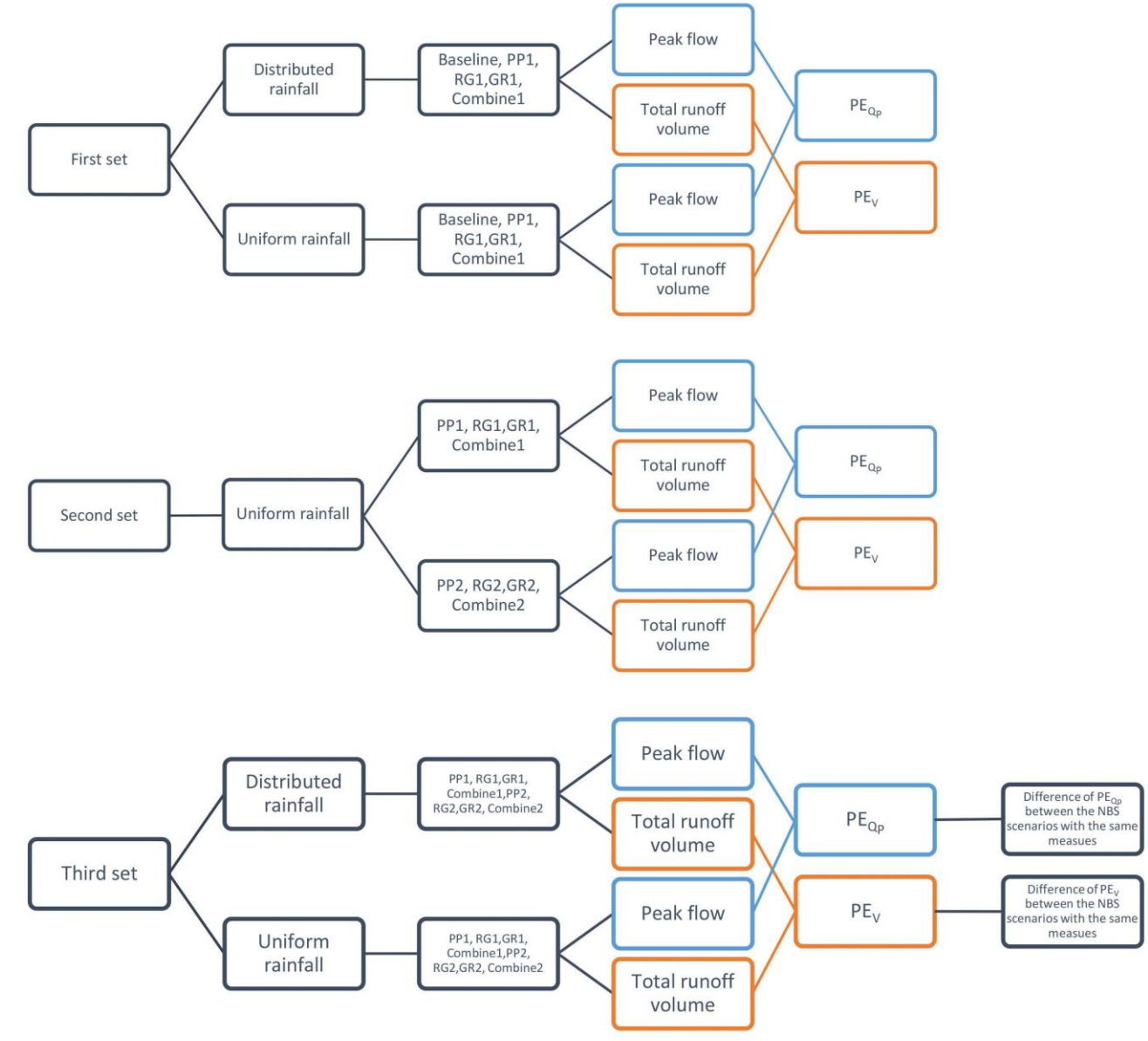

Figure 8: Flow chart of the three sets of modelling experiments.

https://doi.org/10.5194/hess-2020-468
Preprint. Discussion started: 26 October 2020

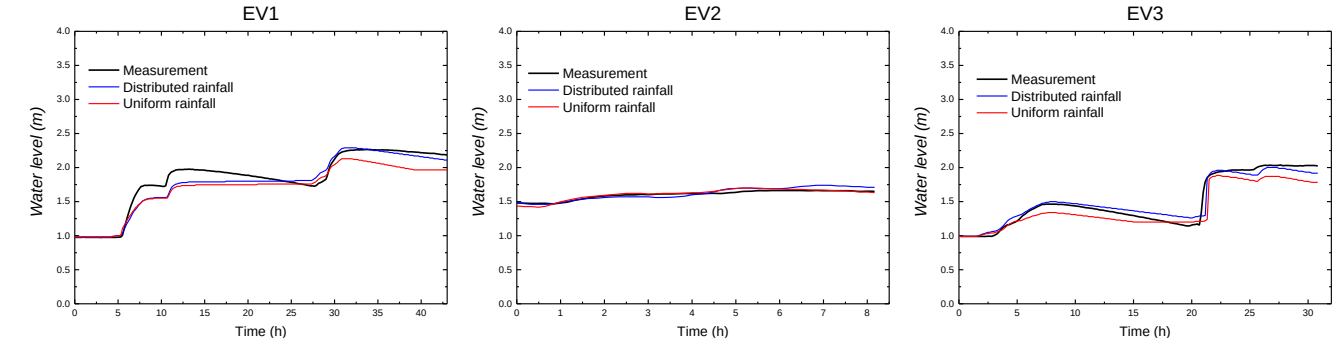

Figure 9: Comparison of the observed and simulated water levels (simulated with distributed rainfall and uniform rainfall) of the three rainfall events.

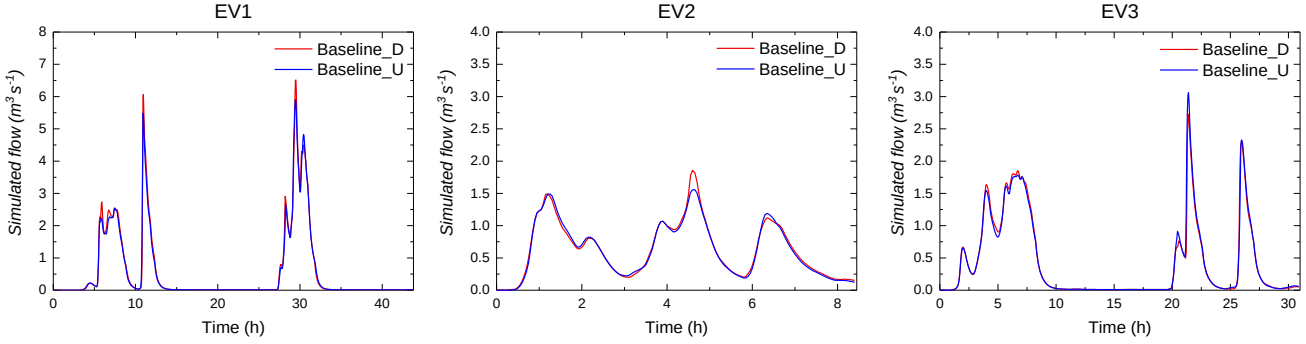

Figure 10: Simulated flow (m^3 s^{-1}) of the baseline scenario under three distributed rainfall events and three uniform rainfall events: (a) EV1, (b) EV2, (c) EV3.

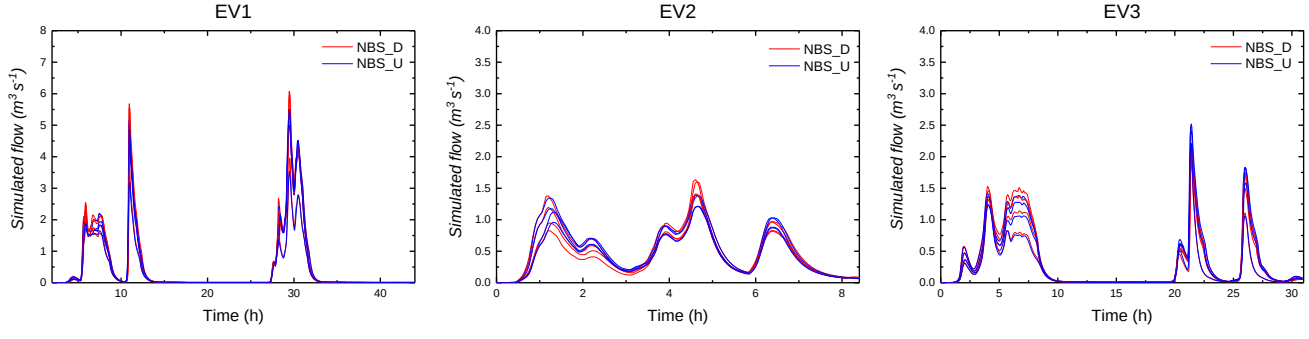

Figure 11. Simulated flow (m^3 s^{-1}) of the first set of NBS scenarios under three distributed rainfall events and three uniform rainfall events (the red hydrographs represent the NBS scenarios simulated with distributed rainfall, and the blue hydrographs represent the NBS scenarios simulated with uniform rainfall).

https://doi.org/10.5194/hess-2020-468
Preprint. Discussion started: 26 October 2020

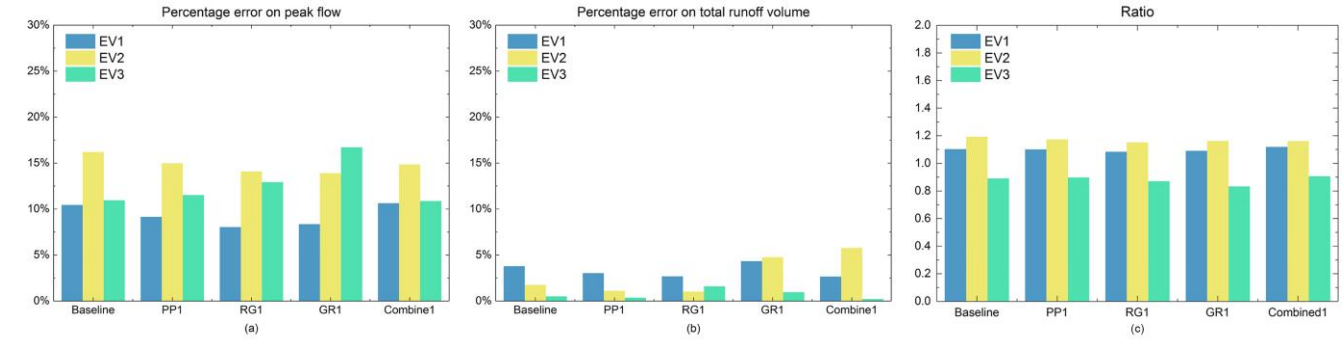

Figure 12. (a) Percentage error on peak flow of the baseline scenario and the first set of NBS scenarios under the three distributed rainfall events and the three uniform rainfall events. (b) Percentage error on total runoff volume of the baseline scenario and the first set of NBS scenarios under the three distributed rainfall events and the three uniform rainfall events. (c) The ratio of peak flow between the scenarios under the distributed rainfall and the scenarios under the uniform rainfall.

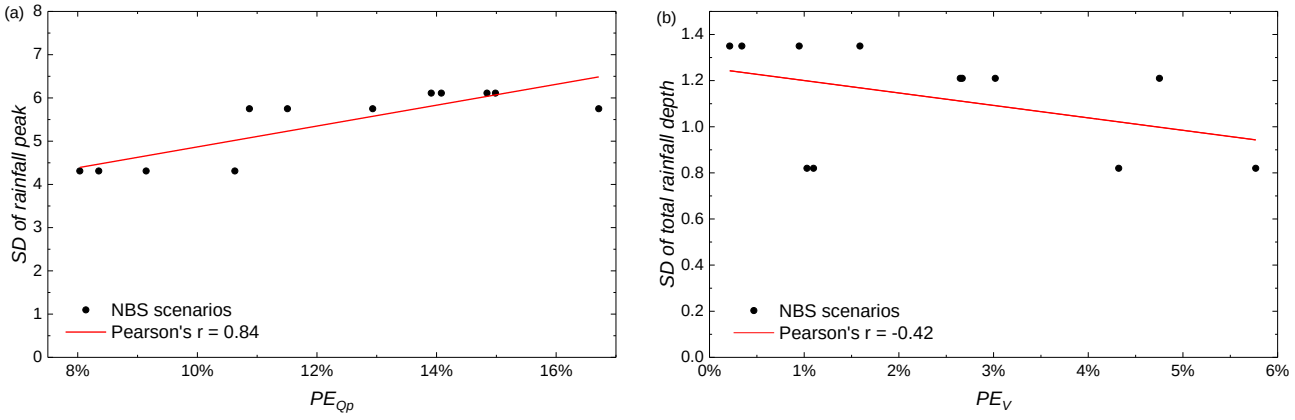

Figure 13. (a) Relationship between the *SD* of rainfall intensity at the largest rainfall peak and PE_{Qp} of NBS scenarios. (b) Relationship between the *SD* of total rainfall depth and PE_V of NBS scenarios.

https://doi.org/10.5194/hess-2020-468
Preprint. Discussion started: 26 October 2020

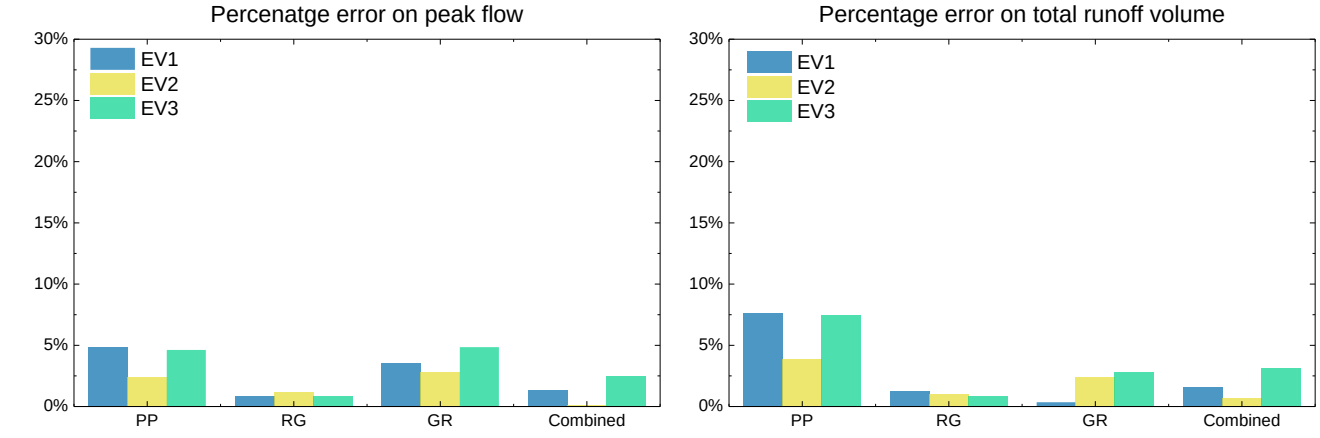

Figure 14. (a) Percentage error on peak flow between the same types of NBS scenarios under the three uniform rainfall events. (b) Percentage error on total runoff volume between the same types of NBS scenarios under the three uniform rainfall events.

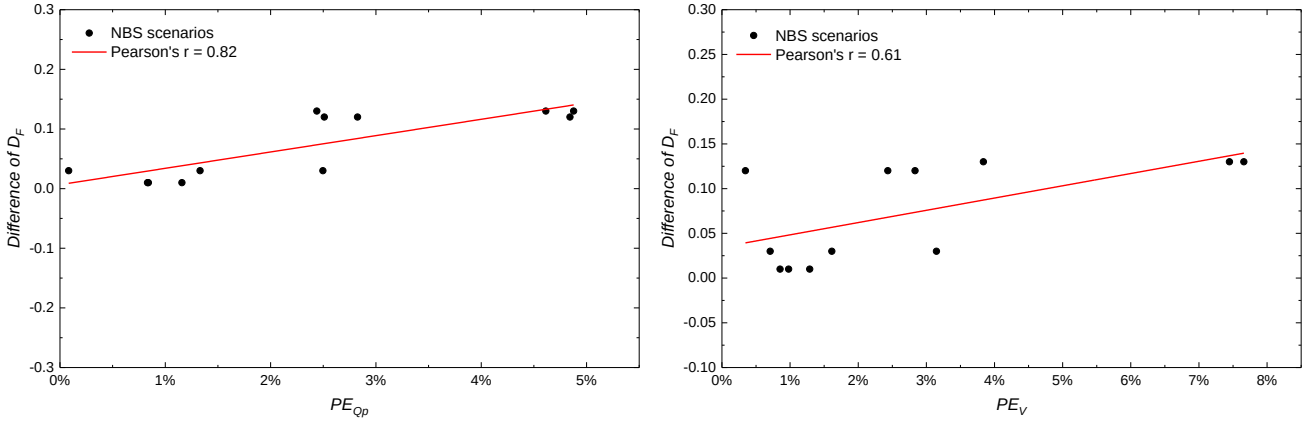

745

Figure 15. (a) Relationship between the difference of D_F of the same types of NBS scenarios and PE_{Qp} of the same types of NBS scenarios. (b) Relationship between the difference of D_F of the same types of NBS scenarios and PE_V of the same types of NBS scenarios.

https://doi.org/10.5194/hess-2020-468
Preprint. Discussion started: 26 October 2020

Hydrology and Earth System Sciences
Discussions
Open Access
EGU

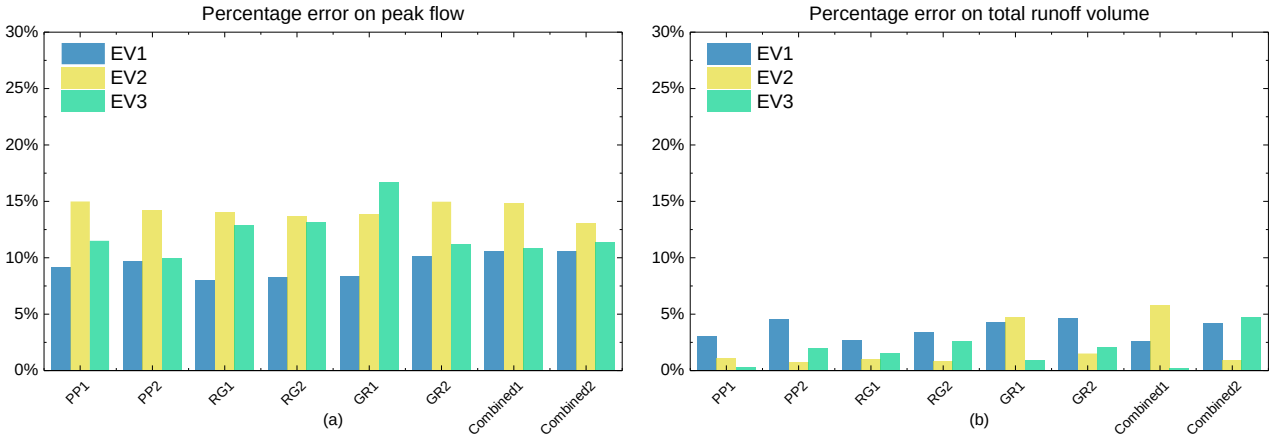

Figure 16. (a) Percentage error on peak flow of all NBS scenarios under the three distributed rainfall events and the three uniform rainfall events. (b) Percentage error on total runoff volume of all NBS scenarios under the three distributed rainfall events and the three uniform rainfall events.

https://doi.org/10.5194/hess-2020-468
Preprint. Discussion started: 26 October 2020

Hydrology and Earth System Sciences
Discussions

Table 1. Main characteristics of selected rainfall events and standard deviation (*SD*) of the rainfall intensity at the largest rainfall peak and the total rainfall depth of the three rainfall events.

Event ID	EV1	EV2	EV3
Data	12-13/09/2015	16/09/2015	05-06/10/2015
Duration (h)	44	8.4	31
Total depth (mm) (areal average/pixel min/pixel max)	31.5/27.4/36.9	12/10.43/14.1	20/17.6/25.4
Max intensity (mm h^{-1}) over 1 min (areal average/individual pixel)	20.5/41.2	9/29.1	36.4/55.6
SD of rainfall intensity at the largest rainfall peak (mm h^{-1})	4.31	6.11	5.75
SD of total rainfall depth (mm)	1.21	0.82	1.35

780 **Table 2. Hydrological parameters for each land use class.**

Land use	Manning's coefficient (no units)	Hydraulic conductivity (m s^{-1})	Interception (mm)
Roads	0.012	1.0e-10	1.9
Houses	0.012	1.0e-10	1.9
Gullies	0.9	1.0e-0	0
Parking	0.012	1.0e-10	1.9
Grass	0.15	1.9e-6	3.81
Forest	0.8	1.9e-6	7.62
Water	0.9	1.0e-0	100
Porous pavement	0.014	1.0e-4	2.14
Rain garden	0.2	1.9e-5	7.62
Green roof	0.14	3.3e-4	3.81

https://doi.org/10.5194/hess-2020-468
Preprint. Discussion started: 26 October 2020

Hydrology and Earth System Sciences
Discussions

Table 3. The details of simulation: NBS scenarios.

NBS measure	Scenario	Proportion of implementation in whole catchment / selected area (after rasterization)	D_F of NBS in small scale/ large scale (after rasterization)	Description of scenario
Porous pavement (PP)	PP1	8.0 %/13.8 %	1.14/1.92	Porous pavements were implemented on the non-driveways (width equal and less than 2.5 m) and some parking lots.
	PP2	8.0 %/10.1 %	1.21/1.79	Porous pavements were implemented on secondary driveways (width between 2.5 m to 5 m).
Rain garden (RG)	RG1	8.2 %/6 %	0.93/1.77	The low elevation greenbelts around houses were implemented by rain gardens, which can collect and store up the surface runoff from surrounding impermeable areas before infiltration on site. When rain garden saturated, the redundant surface runoff will drain into the drainage system.
	RG2	8.2 %/7 %	1.04/1.78	The low elevation greenbelts around public buildings and parking lots.
Green roof (GR)	GR1	8.6 %/13.5 %	1.18/1.87	Small and light green roofs consisting of a soil layer and a storage layer are implemented on all flat roofs.
	GR2	8.6 %/6 %	1.05/1.75	Impervious roofs with slightly slope (≤ 15°) were converted to small and light green roofs (Stanic et al., 2018).
NBS combinations	Combined1	24.8 %/38.5 %	1.59/1.95	A combination of PP1, RG1, GR1
	Combined2	24.8 %/30.4 %	1.45/1.98	A combination of PP2, RG2, GR2

785

https://doi.org/10.5194/hess-2020-468
Preprint. Discussion started: 26 October 2020


Hydrology and Earth System Sciences
Discussions

790 **Table 4. *NSE* coefficients and *PE* values of baseline scenario under the three distributed rainfall events and three uniform rainfall events.**

Event ID	Distributed rainfall		Uniform rainfall	
	NSE	*PE* (%)	*NSE*	*PE* (%)
EV1	0.926	4.6	0.824	7.9
EV2	0.929	2.2	0.948	1.96
EV3	0.954	3.9	0.865	6.9